Assessing the Potential Danger of Hail Impacts on Stiffened Carbon Fiber Composite Panels in Aircraft Structures

L.O.J. Smit

Assessing the Potential Danger of Hail Impacts on Stiffened Carbon Fiber Composite Panels in Aircraft Structures

by

L.O.J. Smit

to obtain the degree of Master of Science
at the Delft University of Technology,
to be defended publicly on Friday August 25, 2023 at 9:30 AM.

Student number: 4479467
Thesis committee: Dr. ir. René Alderliesten, Supervisor
Dr. ir. John-Alan Pascoe, Examiner
Prof. Dr. Christos Kassapoglou, Examiner

Preface

Finishing this project means the end of a long process with many ups and downs, both personal and academic. While this is an achievement I have accomplished, I could not have done it on my own. I want to thank my friends and family who have been continuously walking the tightrope between subtly nudging me forward and not always asking about my progress. All of your support and acceptance has truly helped me through the difficult times in this process. Also, I would like to thank my supervisor, René, for his patience and his positive attitude as well as the many insights he has given during the project.

Abstract

This study evaluates the potential danger of hail impacts on stiffened composite aircraft structures. Test specimen are created using Carbon Fiber Reinforced Polymer (CFRP) with and without an Aluminium longitudinal stringer. These specimen are first indented to explore the effect and behaviour of stiffening elements and varying boundary conditions. Then an impact gun is used to impact the specimen with ice balls, simulating hail impacts in order to assess the potential danger of hail stones impacting the stiffened structure. It is concluded that the critical locations for damage formation are where deformations are most suppressed, such as the stringers and ribs of the aircraft. In these locations more damage at the same energy levels as well as a lower threshold energy level for damage initiation is observed. Additionally, it is shown that repeated impacts in close proximity of each other, such as during hailstorms, can increase the resulting damage compared to separate single impacts. Ice impacts demonstrate only a fraction of the kinetic energy is absorbed during an impact, but large hailstones occurring during rare hailstorms can definitely cause serious damage in the critical locations in aircraft. So, for future research, testing and certifying the potential of hail impacts must be recognised and determined in the critical stiffened locations within an aircraft.

Contents

1 Introduction

In the pursuit of creating lighter and more efficient aircraft, the Airbus A350 and the Boeing 787 have been developed and have been flying since 2013 and 2009, respectively. Over 50% of both of these aircraft their weight is comprised of composite materials, such as Carbon Fiber Reinforced Polymer (CFRP), including the fuselage and wings [3] [12]. The specific strength of these composite materials allow for lighter structures, which is one of the main driving design factors in aviation[1].

One of the disadvantages of CFRPs is their vulnerability to out-of-plane impacts, in part because of their increased stiffness compared to metals. Where metals can absorb energy from an impact by deforming elastically and plastically, a composite will not deform plastically and will strongly resist deforming elastically. As a result, the impact energy is more prone to be absorbed in the form of damage [21]. This makes aircraft susceptible to impacts such as hail storms, tool drops or bird strikes. In addition to this susceptibility to impact damage of composite materials, the damage from impacts will mostly form internally with very little signs of damage from the outside [5]. This Barely Visible Impact Damage (BVID) poses a great threat to aircraft as without proper inspection the integrity of the structures might have greatly reduced with hardly any signs on the outside.

Despite the potential risk impacts bring to aircraft, the current research on this subject is seriously lacking. It is known that the stiffness of composite materials increases the potential damage as deformation is suppressed. Yet, most research on impact damage on composite materials is done on unstiffened panels, while almost all panels in an aircraft will have been reinforced by stiffening elements such as stringers and ribs, further increasing the stiffness of the structure. Additionally, most research is done performing a single impact, while in actuality multiple impacts might occur close to each other during events such as hail storms. As for hail storms, the behaviour and potential threat of ice impacts has also not been comprehensively researched, let alone on a stiffened composite panel.

This study aims to fill this gap in the current research. The research will provide an insight on the effect of stiffening on a composite panel and the corresponding critical locations of an aircraft when subjected to impacts. Additionally, the risk of repeated impacts and ice impacts from hail storms is evaluated. This research is conducted with the use of several experiments. Indentation tests are performed assessing the effect of stiffening and potential of repeated impacts after which a gas gun is used to impact the stiffened CFRP panels with ice spheres determining the behaviour and threat that hail storms pose to the aircraft of now and the future.

2

Literature Review

2.1. Damage Morphology

This section describes the way composite materials react to impacts and the way damage is formed. The main failure modes as a result of an impact are delaminations, matrix cracking and fibre failure [22]. These are discussed in the following subsections as well as the propagation of damage through a laminate.

2.1.1. Delamination

Delaminations are the separation of different lamina. It has been shown experimentally that these occur at the interface of lamina with different fibre orientations[1] [22]. It was determined that delaminations are caused by the mismatch of bending stiffness between plies, so the greater the mismatch, the greater the delaminated area, with the worst case scenario being the interface between 0 and 90 degree plies [22]. Delaminations are of a major concern as these significantly lower the residual strength of materials[1]. As a result of impact, these delaminations often have the oblong shape of a peanut, with the large axis following the fibre direction of the ply below the interface, when impacted on the top surface. In reality though, the shapes of delaminations are far more irregular and a clear direction is not easily determined[1].

2.1.2. Matrix cracking

Matrix cracks are generally the first type of damage to take place during an impact [22]. The cracks can occur throughout the matrix as well as in the bonding between fibre and matrix. Matrix cracks by themselves do not directly lead to significant reduction of strength, however these cracks do lead to delaminations. This can be seen in Figure 2.1 in the transverse view. When the matrix cracks in the upper layer reach the interface, propagation into the other layer is prevented by a mismatch in fibre direction, so the crack continues between the interfaces, as a delamination. Similarly, the shear crack in the bottom layer results in the separation of the bottom two layers[22].

The two main forms of matrix cracks are presented in Figure 2.2. The top image shows shear cracks. These are generated by the shear force as a result of the transverse force applied by the impactor. As a result they are usually at an angle of 45 degrees. The bottom image shows an example of a tensile crack. These occur when the transverse tensile strength of the lamina is exceeded due to the bending stresses during the impact [1].

2.1.3. Fibre failure

Fibre failure is generally one of the last failure modes to happen. It is also one of which the least is known [1]. Not much is known about this failure mode as the focus of research has been on low-energy impacts whereas fibre failure occurs mainly at higher energies [22]. One study by Avery and Grande [6] has identified the fibre damage per ply after an impact. It was found that the fibres in the top layers are damaged as a result of locally high stresses and indentation effects and the lower plies are damaged as a result of the bending stresses [22].

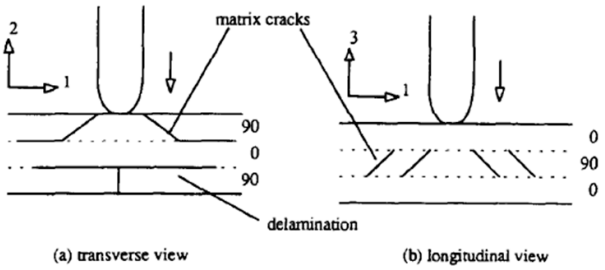

Figure 2.1: Delamination and matrix cracks after impact [22]

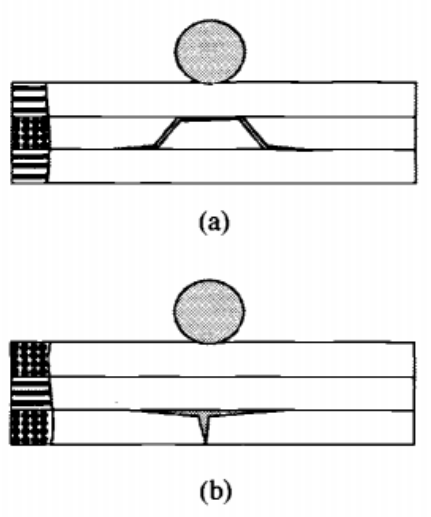

Figure 2.2: Matrix cracks (a) shear cracks (b) tensile crack [1]

2.1.4. Propagation

Another aspect of damage formation of composite laminates is the location where damage is initiated and how it propagates through the thickness. This is described by Abrate [1] and presented in Figure 2.3. With thick laminates damage is initiated at the location of the impact because of the high local contact forces. Then the damage progresses down through matrix cracks and delaminations, resulting in a ”pine tree pattern”. For thin laminates, on the other hand, the damage initiates at the back of the panel as a result of the bending stresses. Similarly, the damage progresses upwards through cracks and delaminations forming an upside down pattern of the thick laminates.

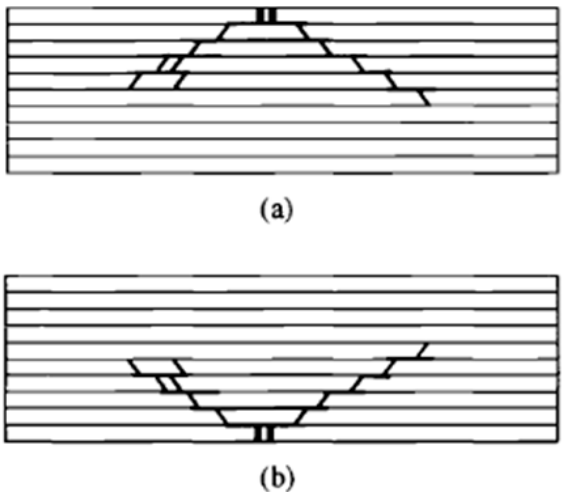

Figure 2.3: Damage propagation of matrix cracks and delaminations in (a) thick and (b) thin laminates [1]

2.2. Damage detection

An important part of assessing the damage caused by impacts and other sources of damage is evaluating the damage within the laminate or structure. In this section several techniques are presented and discussed, both non-destructive and destructive.

2.2.1. Non-destructive inspection

The easiest and cheapest form of non-destructive testing is to simply determine damage visually. There are many types of visual inspections such as a general walkaround, detailed visual or special detailed visual inspections [7]. In general visual inspection is an efficient way to spot larger damages such as surface cracks, paint damage or loose or missing bolts. However, the spotting of damage visually is limited. If no damage is seen by the naked eye, damage could still be present within the structure. Similarly, even if damage is spotted, the extent of the damage is not known precisely. So, visual inspection can be used to find signs of damage after which other techniques can be used to assess the extent and effect of the damage.

The mostly used technique to determine internal imperfections, such as delaminations is using ultrasonic inspection. Ultrasonic inspection works by emitting high frequency sound waves and capturing the reflected waves. The way it works is presented in Figure 2.4. When no flaw is present in the material a single echo peak is received. However, when a crack or delamination is present the perceived this produces an echo that is faster than the back surface echo as the distance is shorter.

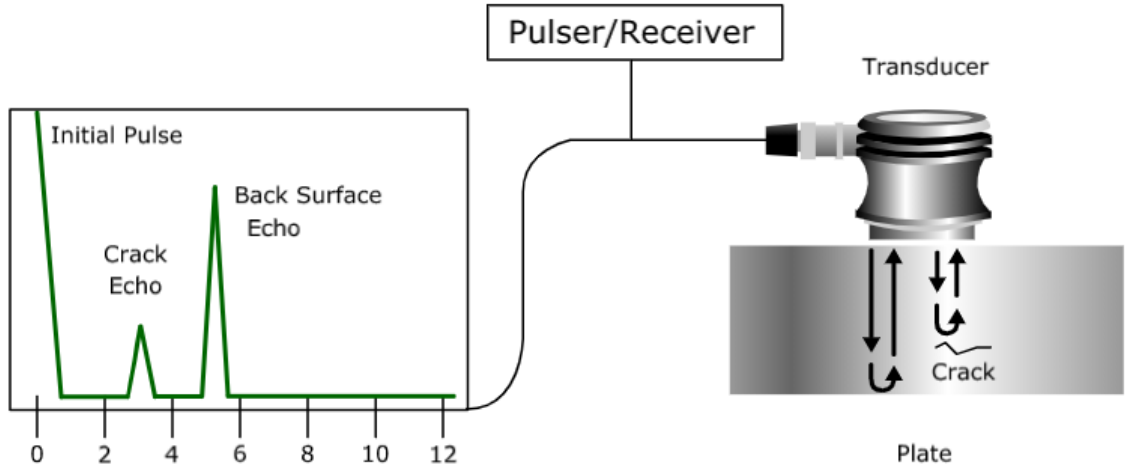

Figure 2.4: Received signal with corresponding material [13]

Another form of ultrasonic testing is called a C-scan. This is the same principle of ultrasonic testing but then it is over a certain area of the part instead of a single location. A C-scan is made by doing scans as presented in Figure 2.4 over the interested area.

2.2.2. Destructive inspection

One of the disadvantages of non-destructive testing presented in the previous subsection is that while it can be seen how large the damaged area is, information over how the damage is spread through the thickness is not retrieved. For this, one would have to look at the cross-section where the damage is. This is of course not viable for an aircraft in operation to evaluate the damage, however for research purposes it is useful to section strips of a panel and inspect the cross-section. This can then be done by creating microscopic images that can identify the individual layers and corresponding cracks and delaminations.

An example of such an image is given in Figure 2.5 of the location of an impact. With ultrasonic testing it would have been found that a delamination existed, however only the top one would have been found as the waves did not propagate through the delaminations. So, destroying the material can give a better understanding of the damage as a result of an impact.

Figure 2.5: Microscopy image of location of impact [26]

2.3. Previous research

This section describes previous research that is performed on the impact response of composite materials.

2.3.1. Repeated impacts

The danger of repeated impacts lies in the fact that after an initial impact, the weakened structure is more prone to damage when impacted again. Alternatively, if a first impact already caused damage, this damage could have reduced the resistance to further damage causing increased damage under repeated impacts. First research describing repeated impacts on the same location are presented after which repeated impacts on multiple locations are discussed.

Single location

With hail, many impacts will take place on the structure, many of which will strike in close proximity of each other. Especially when an initial impact causes damage, the possibility might open up for a second impact to further reduce the structural integrity.

In order to analyse the effect of subsequent impacts, it is helpful to inspect the results of the first impact. In the research by Bienas et al. [15] thin laminates of CFRP and GFRP are subjected under repeated impact to identify the impact resistance of both materials and the effect of repeated impacts in the same location. laminates of 1.5mm are impacted one, three and five times with 5J impacts. Macroscopic images of the damage are shown in Figure 2.6. It was concluded that after the first impacts on the CFRP only damage on the inside was created in the form of delaminations and matrix cracks, while only showing BVID on the outside. After the fifth impact this internal damage did spread to the outer layer, showing a visible crack. The GFRP, on the other hand, showed obvious signs of damage on the outside after the first impact mainly due to the transparency of the material. Additionally, the damage area did not increase as much for the GFRP, which is also shown in Figure 2.7 with the summarised damage area growth. The figure shows how after the first impact the GFRP damage area did not increase as drastically as within the CFRP. It was concluded that it was the stiffness of the CFRP that caused the material to be less resistant to impacts.

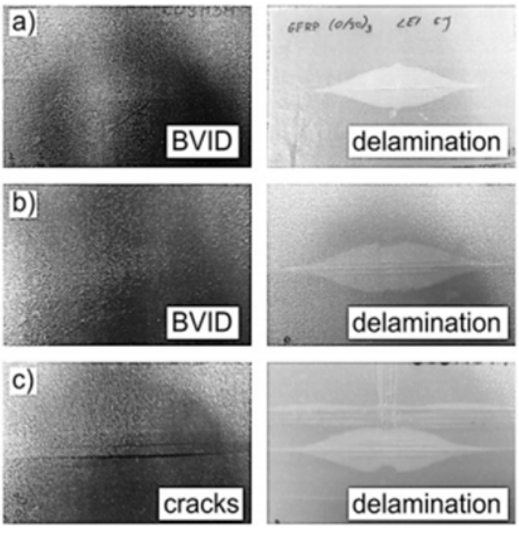

Figure 2.6: Macroscopic images of damage on CFRP(left) and GFRP(right) after (a) 1 impact, (b) 3 impacts and (c) 5 impacts [15]

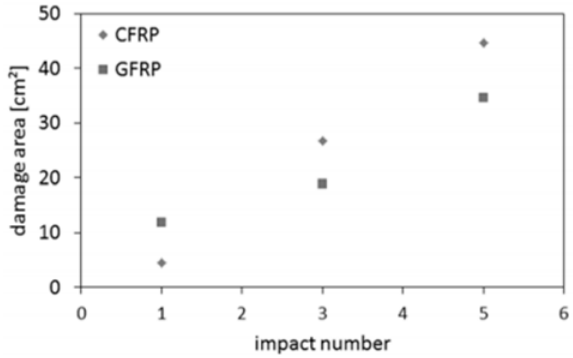

Figure 2.7: Damage area growth per impact number [15]

Overall the conclusion of the research were that the composite materials showed limited resistance to impact damage, with the CFRP showing the lowest resistance. Additionally, it showed that the forms of damage propagation were the same as the forms of damage initiation, being delaminations and matrix cracking. The final conclusion was that the damage propagated in the fibre direction, so damage is dependant on the properties of the composite and the individual layers [15].

It was seen that the damage increased with repeated impacts, but no more than five impacts were performed per panel. So to fully understand the effect of repeated impacts in a single locations more impacts are required. Laminates of 32 plies, with a thickness of about 4mm, are impacted repeatedly with impacts of 15J until penetration occurs in a study by Liao et al. [4]. For this research the effect of impactor diameter is also investigated, by varying the diameter between 10,12,14 and 16mm. A graph showing the damage area growth for all impactors per impact number is shown in Figure 2.8. It can be seen that the damage area increases significantly during the first couple of impacts after which a plateau is quickly reached and the area stays relatively constant until penetration. Additionally, while the larger impactors cause a larger area to be damaged, the number of impacts required for penetration also goes up while the impact energy remained constant at 15J for each impact. Furthermore, C-scans are presented for the panels impacted by the 10 and 16mm impactor in Figure 2.9. In the figure the damage area can be compared between the two impactor, where it can be seen that the impactor with a diameter of 16mm causes a larger damage area from the first impact onward. This is mostly expected as the area of the impactor is simply larger as well. So, also the energy of the impact is spread over a larger area which explains why the smaller impactors result in penetration with fewer impacts. All in all, the research shows how the damage of repeated impacts on the same location is limited to an area around the impact dependant on the size of the impactor as the damage area reaches a plateau until penetration. These results would suggest that repeated impacts in a single location are not that critical as the majority of the damage will have been formed after two or three impacts.

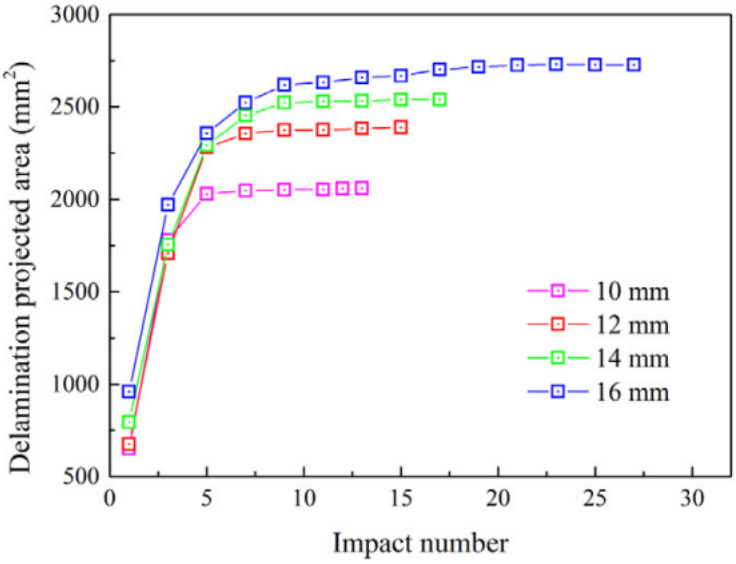

Figure 2.8: Damage area growth per impact number for all impactor diameters[4]

These findings are similar to the conclusion found by Verstraeten [26]. The effect of impact fatigue was evaluated in the research by impacting a thin laminate on the same location with impacts of 6J. A total of 225 impacts were performed. The results are shown in Figure 2.10, with a fitted curve on the left and the measured date on the right in the table. Especially interesting in these findings is how fast the damage area growth rate decreases with repeated impacts. The first impact does three times as much damage area-wise than the next four impacts combined. Similar to the research by Liao et al.[4] the area increases quickly in the first impacts after which a plateau is approached.

In addition to the damage area, the cross-sections of panels subjected to repeated impacts have been observed to evaluate the damage through the thickness. Microscopic images of three cross-sections are presented in Figure 2.11. These are three different panels cut by hand through the impact location, hence the second panel was not cut perfectly through the damage which is why the damage is less after five impacts compared to one impact. The images show how the width of the damage growths with repeated impacts and how the delaminations leap between layers causing wide delaminations in those layers as well.

Interestingly it was concluded overall by Verstraeten that two impacts in two separate locations will

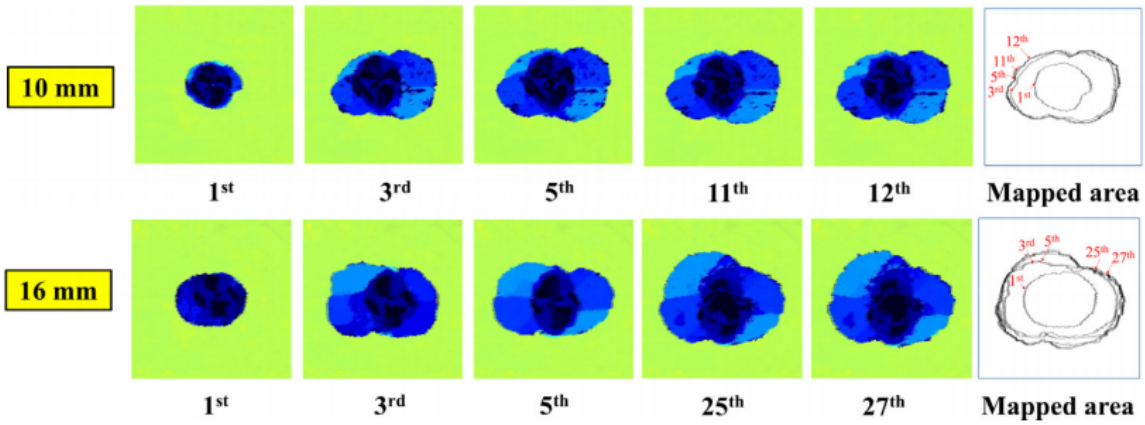

Figure 2.9: C-scan results of delaminated areas after repeated impact by impactor diameter of 10 and 16mm [4]

cause more internal damage than five impacts in the same location, thus also affecting the structural integrity more with these two impacts. This is an important conclusion for future research concerning the damage of hail impacts as hail is a phenomenon that will inherently result in repeated impacts in multiple locations, so this must be accounted for as well in the structural testing.

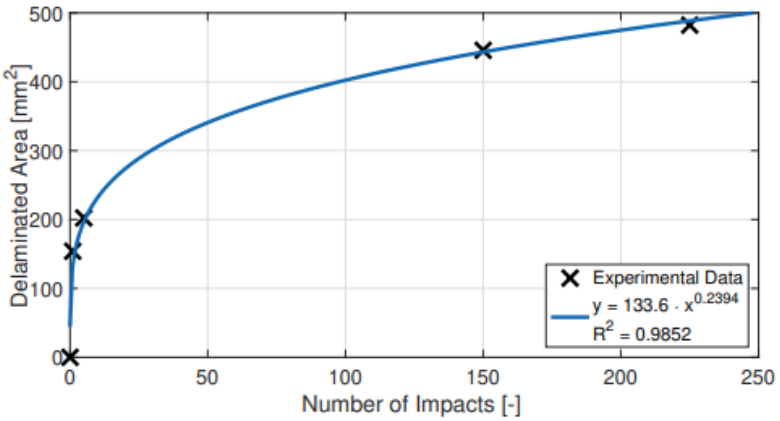

Impact Number [-]	Area [mm^2]
0	0.0
1	154.0
5	202.4
150	445.7
225	482.3

Figure 2.10: Fitted curve of the measured damage areas presented in the table [26]

Multiple locations

As shown in the previous section, the danger in hail impacts might lie in the form of repeated impacts in different locations. Therefor, this section will discuss two cases of research that is performed on the effect of repeated impacts in different locations.

Laurençon [17] set out to assess the response of thin CFRP panels of 8 plies under repeated impacts that were distributed closely together. For the research certain parameters were altered to identify the individual effect of each. Firstly, the impact energy was varied between 2, 4 and 8J for the tests. Secondly, the effect of the number of repetitions was evaluated and finally the distance between the impact locations was varied. The latter was done according to a unit cell set-up as shown in Figure 2.12. Using these unit cells, an impact density is computed to evaluate the effect of spacing.

The effect of the number of repetitions is discussed in more detail. For this discussion the results of a test with a spacing of L=0.015m, according to Figure 2.12 and an impact energy of 4J were used. A graph of the effective damage area per impact number with corresponding C-scan images is presented in Figure 2.13. Initially, the individual impact locations behave as was seen in the research of repeated impacts in a single location. Each location shows a slowly increasing damage area with increasing impact number. However, eventually something happens that has not been seen before. The individual damage areas have increased to a point where they link-up and the total damaged area rapidly increases. So comparing this to the results from the repeated impacts on a single location we see two

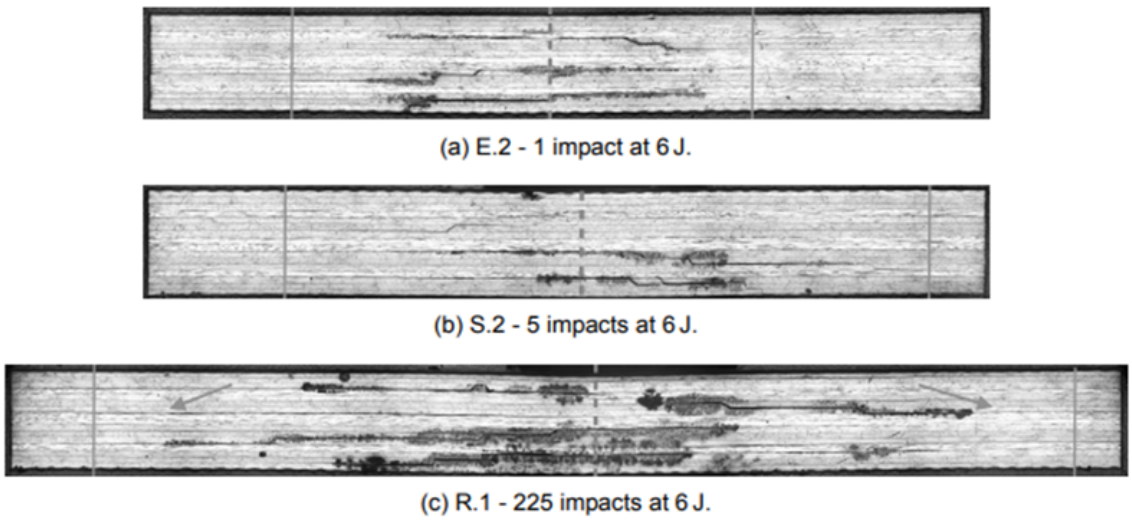

Figure 2.11: Microscopic images of the cross-section after repeated impacts [26]

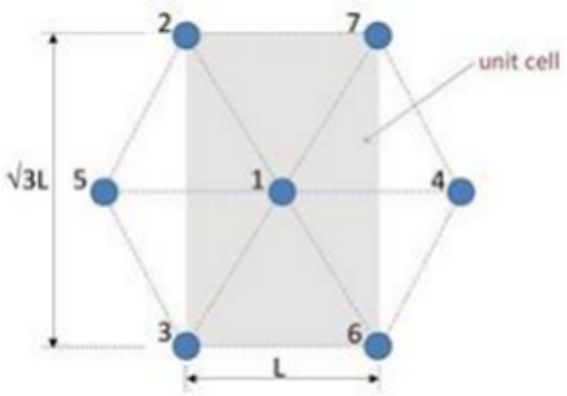

Figure 2.12: Unit cell describing the distribution of impacts on the panel [17]

clear distinctions. First, with a lower number repetitions the damaged area is immediately more significant as in this case there are already seven location with damage after the first location. Second, with a higher number of repetitions link-up could cause a drastic increase in damage in a structure resulting in a sudden decrease in residual strength which could be detrimental to the integrity of the structure.

The main conclusion of Laurençon [17] for the future research that is proposed in this report is that repeated impacts with close spacing could result in more damage with lower energies than if higher energies were used for impacts with a large spacing between impact locations. This is because the link-up between locations will increase the area whereas, as seen before, same location impacts have a limited plateau of damage area around the location of impact.

This phenomenon of link-up has been shown also by Verstraeten [26] in his research. In this research the effect of impact spacing, by varying the spacing between impact locations under repeated impacts. Figure 2.14 shows a C-scan of a panel after three locations have been impacted once with an impact of 15J. The locations have been selected lie along +45 and -45 degrees from the top location. A link-up can be seen along the -45 direction from the top location to the right location. It is concluded that this occurred due to the damage following the fibre direction and not perpendicular to it.

Another test performed was on the effect of spacing of impact locations, similar to Laurençon. For this test five impacts of 6J were performed per location on three locations with varying spacing. C-scans of two panel are presented in Figure 2.15. The left image has a spacing of 30mm between locations, whereas the right panel has a spacing of 15mm between impact locations. It can clearly be seen how

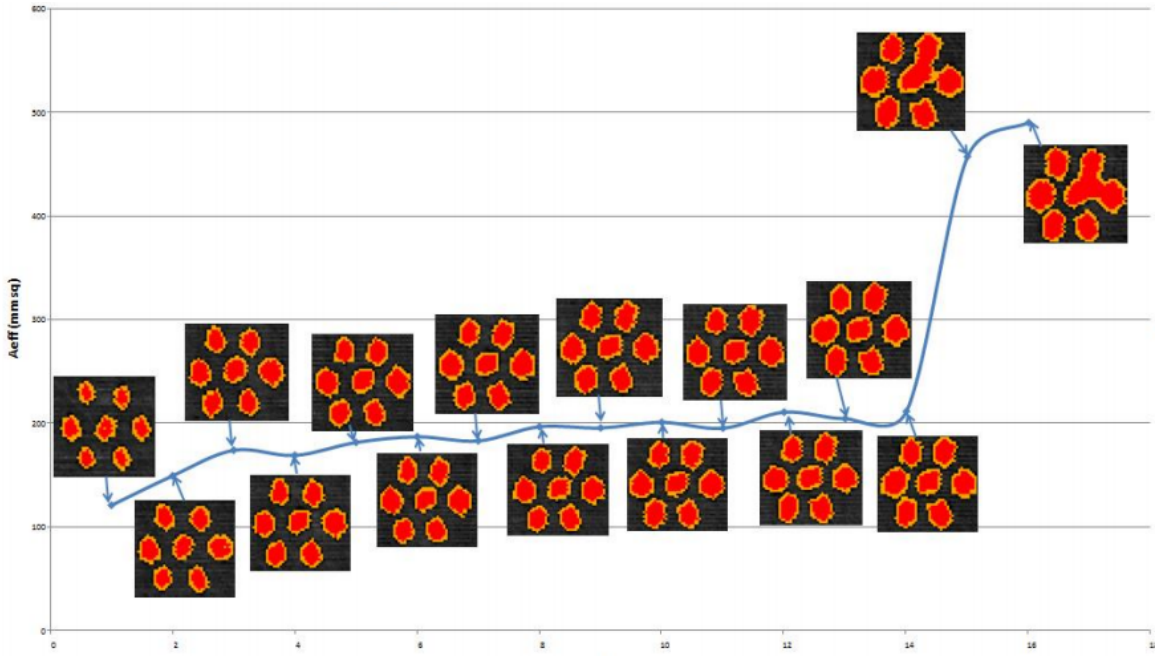

Figure 2.13: Effective damaged area per impact number and corresponding C-scan images [17]

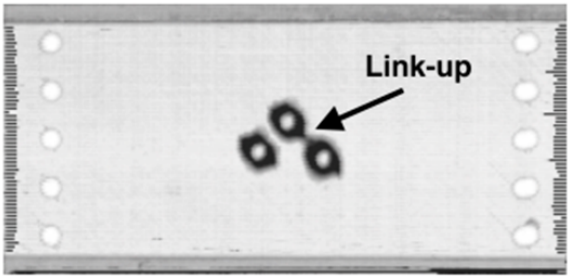

Figure 2.14: C-scan of panel after impact with link-up in -45 direction[26]

the damage area between the impact locations can interact with a small spacing after repeated impacts.

The overall conclusion of Verstraeten on the topic of link-up was that it is clearly a possibility, however even during testing the parameters have to be just right to enable it to happen. If spacing is too far apart no link-up happens and if the spacing is too close then damage areas simply overlap. So he concludes that in order to realistically encounter link-up due to hail a ”one impact per location” philosophy will show a better representation of the real life situation [26].

2.3.2. Stiffened panels

All previous sections show examples of research done on the response of flat unstiffened panels to impact testing. This section discusses the impact response of stiffened panels. Stiffened panels have a higher flexural stiffness and will thus have a higher resistance to deformation.

This is an aspect of impact damage on composite panels that is not covered extensively in literature. The majority of research done on the subject of (hail) impacts on composite structures focus their tests on flat unstiffened panels. However, as mentioned, the danger is that stiffeners prevent displacement causing less energy to be absorbed elastically and more energy absorbed as damage. The previous two subsections have shown that while the increased stiffness can lead to higher peak forces, a low stiffness allows for more deformation which could result in additional damage due to the strain. So, this section will analyse whether the addition of stiffeners will increase the stiffness to such an extent that the panel becomes more prone to damage due to impacts.

First, research by Le [18] is presented. In this study a curved stiffened composite panel is impacted

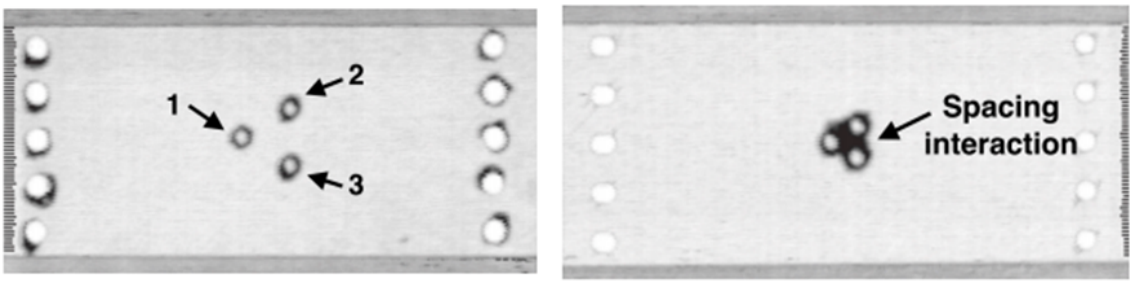

Figure 2.15: C-scans of two panels with different spacing showing interaction between damage areas[26]

at high-velocity with ice balls to evaluate the effect of stiffeners on the damage. The layout of the panel and the impact locations are shown in Figure 2.16. It can be seen that the panel is slightly curved, to represent a fuselage panel, and has hat stringers as well as shear ties, representing ribs.

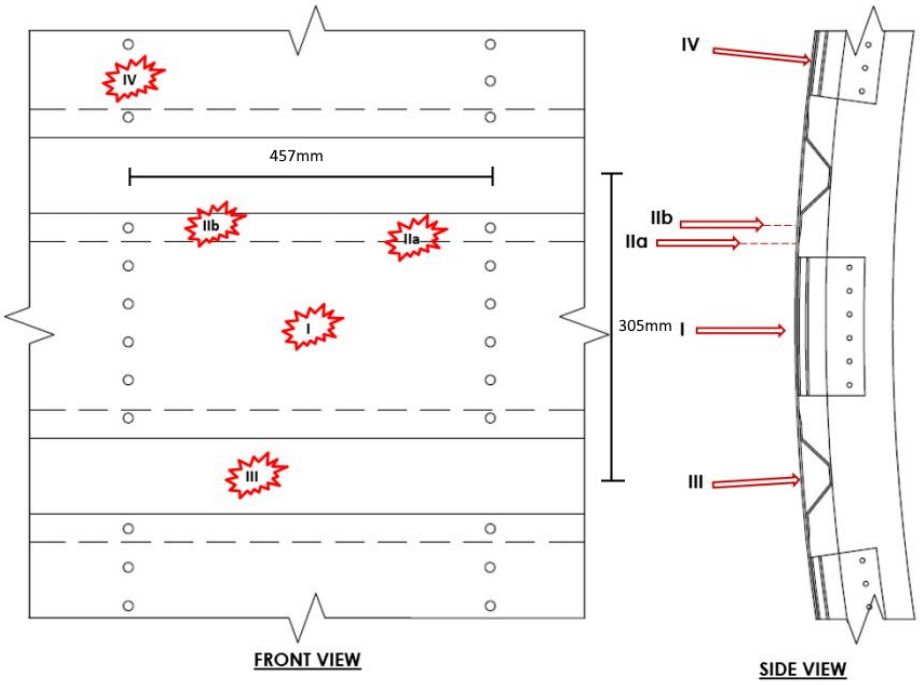

Figure 2.16: Impact locations on the curved stiffened composite panel [18]

In order to evaluate how critical each location is, a baseline failure threshold energy (FTE) is first determined. This is the energy level of an ice ball at which failure occurs. For the baseline a flat unstiffened panel of 305 by 305mm, with the same lay-up, was impacted with an ice ball of the same diameter, resulting in an FTE of 489J. For each impact location a FTE was determined and then compared to the baseline. The results are presented in Figure 2.17.

It was concluded that impacts on the stringer flange were most critical with the FTE at the end of the stringer flange being between 0.1 and 0.3 times the FTE of the flat unstiffened baseline. Also the middle of the stringer flange and the region under the hat stringer are quite prone to damage with a scaling factor of 0.37 and 0.73 respectively. Impacts on the middle of the bay showed a large variance in the results. The scaling factor ranged from 0.46 to 1.16. A reason for this range is given as a varying proximity to the stringer or shear tie. So, while the research showed that for some tests the middle of the bay was less critical than the baseline flat panel, for some tests the scaling factor was as low as 0.46. Thus, even an impact on the middle of the bay, a locally unstiffened panel, could result in increased amounts of damage due to the nearby stiffeners. It should also be noted that differences between the base line and the test results could originate form the differences in set-up. The baseline panel is a

Impact Location	FTE [J]	Scaling factor
I – Middle of bay	227 -567	0.46-1.16
IIa – End of stringer Flange	49– 147*	0.10-0.30*
IIb- Middle of stringer Flange	183	0.37
III – Middle of Stringer	357	0.73
IV – Directly over Shear Tie	563**	1.15**

Figure 2.17: FTE and scaling factor of baseline for each impact location [18]

square panel of 305mm by 305mm clamped on all sides while the panel has a bay with dimensions of 305mm by 457mm clamped by the shear ties and supported by the stiffeners.

Another interesting observation is presented by Le et al. [25] continuing on the research presented by Le on the curved stiffened panel [18]. It was shown that for the impact in the middle of the bay with low energies, damage was not initiated at the location of the impact. Instead, the first signs of damage were seen in the corners of the bay, where the stringers and the shear ties met. This further substantiates the risk of impacts on stiffened panels as the damage can be found in locations different from the impact location.

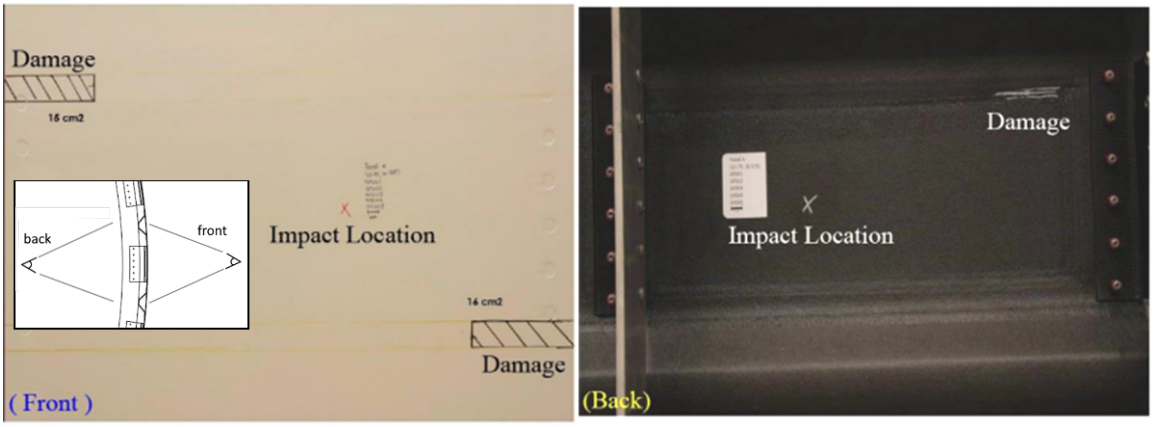

Figure 2.18: Front and back view of impact location and damage initiation sites [25]

To evaluate the reason of damage initiation a finite element method was used to recreate the impact on the structure. It was concluded that the impact caused a stress wave which propagates from the location of the impact. When this wave reached the constraints it was seen that under certain conditions the deformations of the skin and stringer were out of phase due to the differences in stiffness. As a result, delaminations occurred where the deformation of the stringer was prevented due to the boundary conditions set in place by the shear ties. This was verified by running another simulation with the same impact on the same location after removing the shear ties from the structure. This time no damage was caused by the impact. It is therefore concluded that the damage from the impact was due to the discontinuity in stiffness as a result of the stiffener and shear tie [25].

Another research on the effect of stiffeners is discussed of Rout and Karmakar [23]. An FEM is presented to assess the effect of stiffeners on the impact response of a composite shell panel. The unstiffened shell is compared to three models; (A) with stringers in the x-direction, (B) with stringers in the y-direction and (C) with stringers in both directions. The contact force and lateral displacements over time are presented in Figure 2.19. Similarly to what was seen for the curvature and thickness, stiffeners cause a higher contact force and lower lateral displacement as deformation is obstructed. Additionally, model C, with stringers in both direction, shows a slightly higher contact force and smaller displacements. So, as Le et al. [25] have shown, these smaller displacements can result in more damage at the locations of the constraints.

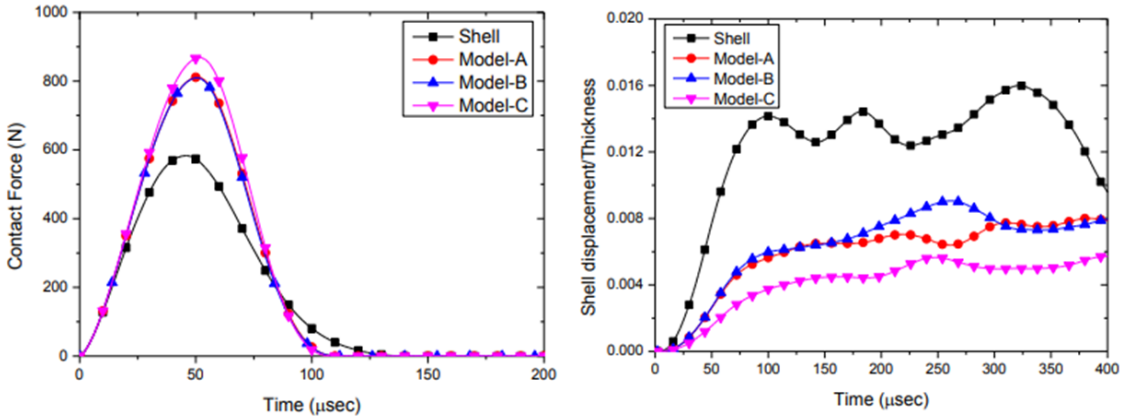

Figure 2.19: Contact force and lateral displacement against time for all models [23]

2.4. Hail

This section gives a brief overview of the characteristics of hail. In order to evaluate the potential danger of hail impacts it is important to understand how hail behaves and how the impacts can be characterised. First, the global distribution of hail is presented. Then, results form hail pads are discussed, after which the physical properties of hail are presented. Finally, the behaviour of ice during impacts is explained.

2.4.1. Location

First, it is important to realise that hail is not an evenly spread problem globally. Some parts of the world are more prone to hailstorms than others. Different studies have been done in order to map the annual hail fall over the world. The difficulty is in the fact that hail is much more likely to be reported in more populated areas, so data voids can exist over less populous regions [9]. However, airports are generally located in more densely populated areas, so reliable data exists for regions where larger airports are located. Court and Griffith have created a map based on reports on the mean annual haildays over the world in 1986. This map is presented in Figure 2.25. The main conclusion drawn was that higher values were seen over mountainous regions.

Another, more recent, map showing the density of hail fall over the world is given in Figure 2.26. The figure shows the density of hailstorms with hail size over 15mm for the months of June, July and August. The overall distribution of hail events is similar as seen on the earlier map, with the largest chance of hail in north America and along Europe and Asia as well as over some mountain ranges. These results show that the problem of hail is not evenly distributed as aircraft flying domestically in Brazil, for instance, will run a far lower risk of hail impact damage than aircraft often landing on airports in the middle of the US.

2.4.2. Hail characteristics

In addition to where hail is to be expected to be most prevalent over the world, it is important to find out the characteristics of the hail that will impact on the aircraft. In this section the size, fallspeed and corresponding energies will be discussed. This information is all required when testing structures on impact as the tests have to be relevant to the real life situation.

Size

First, the size of the hail stones is discussed. A source for hail data is a program called the Community Collaborative Rain, Hail and Snow Network, or (CoCoRaHS). It is a volunteer program that collects hail data around the US. It was set up in 1999 and up until 2014 a total of 22,000 hail pad measurements were reported [11]. So, although the data is retrieved individually by many different people, causing some irregularities, the shear number of data does give a great indication of hail characteristics in real life. The distribution of the maximum hail size for each of the hail pads is given in Figure 2.20. From the data it can be computed that around 80% of the hail stones were smaller than 12.7mm in diameter and 90% were smaller than 25.4mm. This means that around 10% of the hail pads have recorded

a hail stone in size greater than 25.4mm. In addition, Figure 2.21 shows a more detailed distribution of the mean and the maximum recorded sizes of hail stones in percentages. Both the mean and the maximum recorded size per hail pad were mostly between 6.4 and 12.7mm with 60 and 55 percent respectively. Another conclusion from the data is that only about three percent of the hail pads had a mean above 25.4mm. So, while larger hailstones are common, the vast majority of the hailstones are smaller.

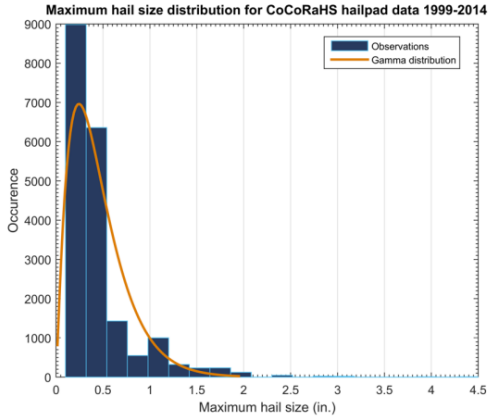

Figure 2.20: Maximum hail size distribution [11]

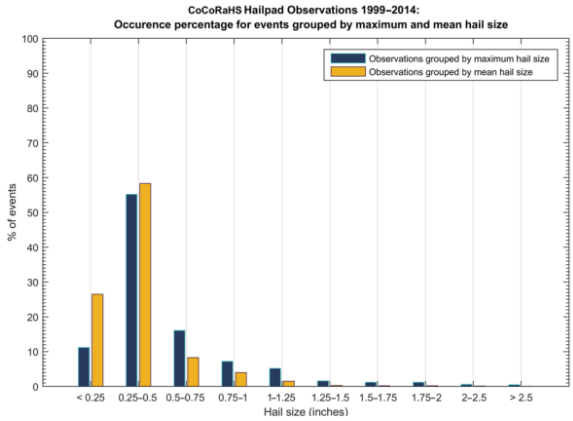

Figure 2.21: Percentage distribution of maximum and mean hail size [11]

Additionally, from the damage tolerance overview of the A350 design program it was stated that the design was based on a meteorological survey. of which the following sizes and distributions were retrieved[19]:

- Standard hailstorms, diameter of 10mm for 50 percent of hailstorms
- Rare hailstorm, diameter of 25mm for 5 percent of hailstorms
- Extremely rare hailstorm, diameter of 50mm for 0.1 percent of hailstorms

So while the numbers do not exactly match up, a very similar distribution is shown to be found by Airbus. Also it should be noted, no information was given by Airbus on the origins of this meteorological survey. It is possible that this data is from Europe as Airbus is located around Europe, while the data from CoCoRaHS is solely from hail pads throughout the US. Alternatively, both the US and Europe could have been taken into account. However, as both sources result in similar distributions, they can be confidently used to evaluate the hail that will be encountered in the lifetime of an aircraft.

Density

With the size distribution known of hail it is important to evaluate the density to obtain the mass distribution of hail. Measurements have shown that hail often does not have the density of solid ice as well as that the density varies significantly [9]. Especially for smaller hailstones the density varies as experiments have shown a density range from 50 to 890 kg/m^3 for hail stones smaller than 20mm, while larger hail stones have a density from 810 to 915 kg/m^3 [9]. Some of the found data is presented in Figure 2.22.

As mentioned, the smaller hailstones have a great variation in density while larger hailstones are more consistently closer to the density of solid ice. However, even a large portion of the small hail stones have been shown to have a density near the density of solid ice. So, it is concluded that it is acceptable to assume the worst-case scenario and assume a density for hail stones of 917 kg/m^3 as solid ice.

Velocity

The next step is to determine the velocity with which the hail stones will impact the aircraft. The velocity of the hail stones are made up out of the vertical velocity, based on the terminal fall velocity, and the horizontal velocity, based on wind conditions. During an oblique impact, only the component normal to

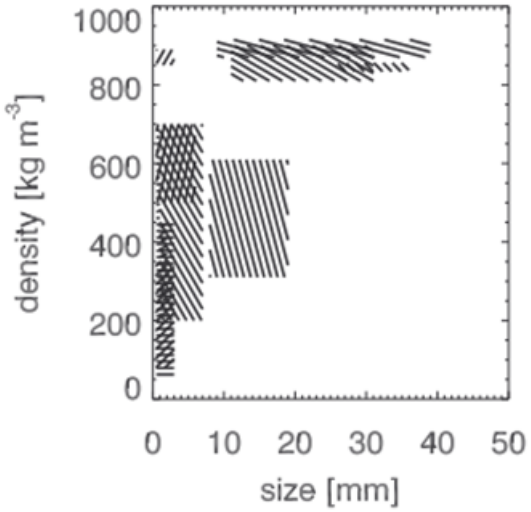

Figure 2.22: Experimentally found relations between density and size [9]

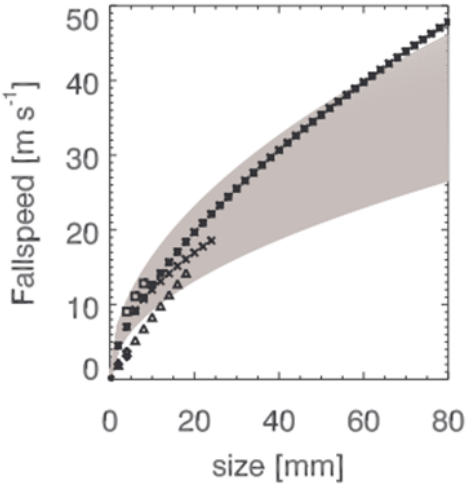

Figure 2.23: Experimental and theoretical results of fallspeed against size [9]

the surface contributes significantly to the impact [10] [16]. So, on top of the aircraft only the fallspeed will be the contributing velocity component.

The terminal velocity, V, for a hail stone falling is given as follows [9]:

$$V = \sqrt{\frac{4g\rho_{hail}D}{3C_d\rho_{air}}} \tag{2.1}$$

Where g is the gravitational acceleration, ρ_{hail} and ρ_{air} are the densities of hail and air respectively, D is the size of the hail stone and C_d is the drag coefficient of the hail stone. The drag coefficient of hail is not as easily determined as hail stones are not perfect spheres, are almost always differently in shape and have a slightly rough surface [9]. The resulting terminal velocities for a range of drag coefficients is shown in Figure 2.23. The region in grey is between a drag coefficient of 0.5 and 1.5, with the lower drag coefficient causing higher velocities. In addition to this grey area with the theoretical results, some experimental results are plotted as well. So, it can be concluded that for the larger hail stones this drag coefficient of 0.5 is a good approximation.

On top of the fuselage, the terminal velocity is the only component of influence, however the fuselage is curved and hail can impact on the sides as well. This is of importance in the case of horizontal wind, when the hail stone will pick up speed due to the wind and can still hit the fuselage with a large velocity component normal to the surface. Horizontal wind components in hailstorms can typically reach velocities of 10 to 25m/s with gusts up to 50m/s [14]. The effect of this horizontal component is briefly discussed in the next section.

Energy

With the size, density and fallspeed known of hail, the corresponding energy levels can be computed. This is done by evaluating the kinetic energy ($E = \frac{1}{2}mV^2$). Based on the findings of the previous sections, a relation between size and kinetic energy is given in Figure 2.24, with a drag coefficient of 0.5. Two curves are presented, one with only the terminal velocity taken into account and one where a horizontal velocity of 15m/s is added. It should be noted that smaller hailstones will gain more in speed than the larger hailstones from the same wind speeds due to their lower weights. However, it is still a good illustration how hail stones can get a significant increase in energy, over 30% increase at a diameter of 30mm. So, it can be seen that for small hail stones the kinetic energy is relatively low, but the energy increases rapidly with increasing size. Because of this rapid increase in energy it could be the case that the larger hail stones are the biggest threat, even though the majority of hail stones are much smaller.

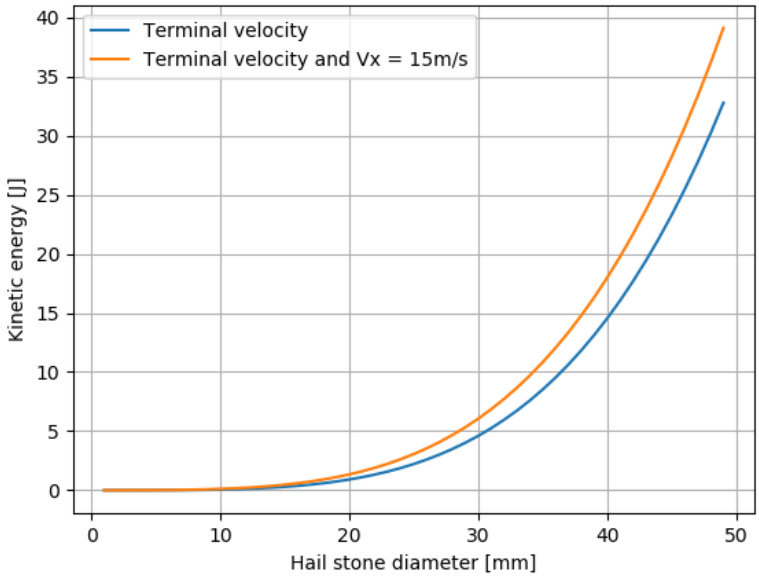

Figure 2.24: Relation between hailstone diameter and kinetic energy

2.5. Research Questions

In this literature review it was shown that for the newer aircraft with a fuselage made out of composite materials a problem could arise when the aircraft was subjected to repeated impacts, such as hail. The stiffened fuselage panel would be repeatedly impacted by hail stones distributed over the fuselage.

Research has shown how two impacts in different locations cause more damage to a laminate than five impacts in the same location. This has been demonstrated multiple times, each time on flat unstiffened panels. Research has shown stiffened panels are more susceptible to damage during an impact. This was determined by several studies, each with a single high-velocity impact. However, no research has been done to evaluate the effect of repeated impacts in different locations on a stiffened panel. Even though research has demonstrated that these factors on their own can cause critical situations, the combination of these has not been put the test.

Future research is therefore required to find out if this situation has been overlooked by research and could result in disastrous consequences as the damage threshold energy might be lower than expected. A typical fuselage panel will previously have been proven to be able to withstand a single impact of a set amount of energy. Now, the question will be answered if this panel, would be able to withstand several impacts distributed around the stiffeners.

In order to answer this question the following research questions are developed:

- What is the effect of stiffening a panel on the response to an impact?
- What is the effect of the distance between impacts on a stiffened panel?
- What is the effect of the distance of impacts to the stiffening elements?
- Can repeated impacts on a stiffened panel influence the energy threshold at which damage occurs?

The answers to these questions could be able to provide the critical locations and situations where impacts are most prone to lead to serious damage, even at lower energy levels.

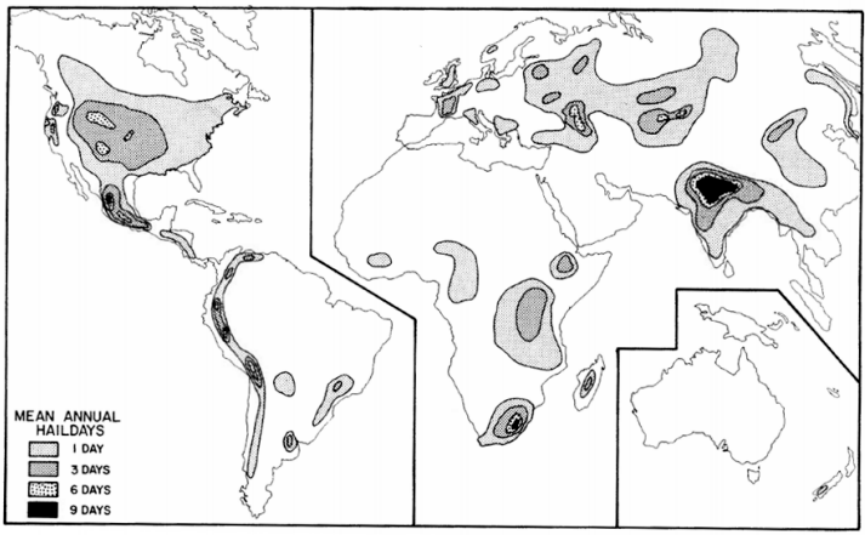

Figure 2.25: Mean annual haildays globally [8]

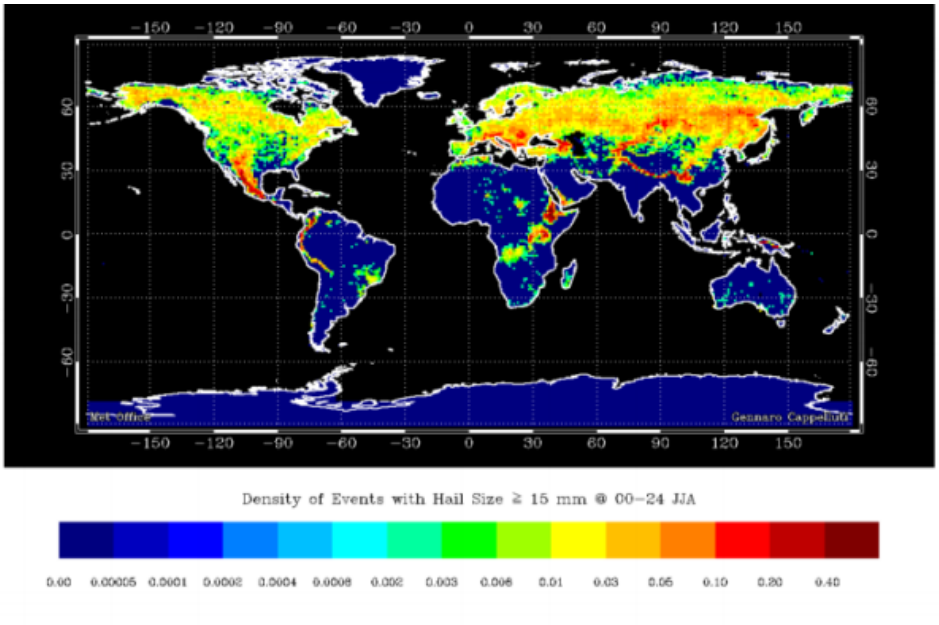

Figure 2.26: Density of events with hail diameter above 15mm [9]

3

Methodology

In this chapter the used methods to answer the research questions proposed in Chapter 2 are presented. First, the design of the specimen is shown. Then, the Set-up used in the testing is given and finally, both the indentation tests and the ice impacts that were performed are presented.

3.1. Test Specimen

3.1.1. Panel design

For the experiments in this study, two different panels have been made. 18 panels with a thickness of 16 plies and 2 panels with a thickness of 8 plies. Both panels were made with the material Deltapreg M30SC-150-DT 120-34F, a carbon fiber prepreg with the mechanical properties as shown in Table 3.1. The layup with 16 plies is [45,0,-45,90,45,0,-45,0]s and the layup for the panel of 8 plies is [45,0,-45,90]s. So, both panels are symmetrical and balanced, with the thinner panel also being quasi-isotropic. The final panels used were cut to 280mm by 140mm, with the 0° coinciding with the longer side.

Mechanical property	Value
Tensile Strength (0°) [MPa]	3010
Tensile Modulus (0°) [GPa]	145
Tensile Strength (90°) [MPa]	39
Tensile Strength (90°) [GPa]	6.4
Compression Strength (0°) [MPa]	1020
Compression Modulus (0°) [GPa]	133
Compression Strength (90°) [MPa]	138
Compression Modulus (90°) [GPa]	8.1
In-Plane Shear Strength [MPa]	95.6
In-Plane Shear Modulus [GPa]	3.4

Table 3.1: Mechanical properties of Deltapreg M30SC-150-DT 120-34F

3.1.2. Stiffener design

For the stiffener along the panel it was decided to use Aluminium and attach the stringers to the CFRP panel using an adhesive. This would greatly reduce the labour, time and money compared to co-curing or co-bonding a CFRP stiffener in an autoclave. A simple flat stiffener was created by forming two Aluminium strips of 1mm into L-profiles and gluing them together and onto the panel as shown in Figure 3.1. For the adhesive Scotch Weld Epoxy Adhesive 2216 B/A is used. The complete panel including stiffener is then as presented in Figure 3.2.

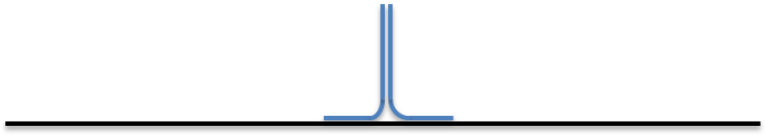

Figure 3.1: Flat stringer created by joining two Aluminium L-profiles

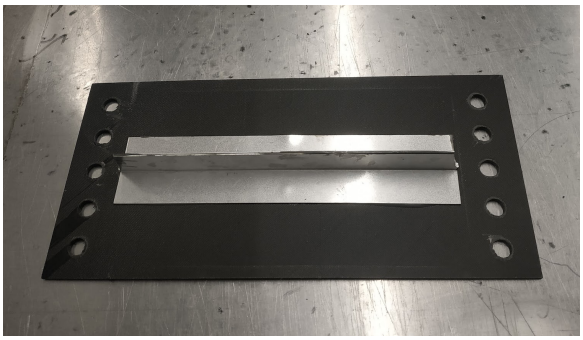

Figure 3.2: Manufactured panel with Aluminium stiffener and bolt holes

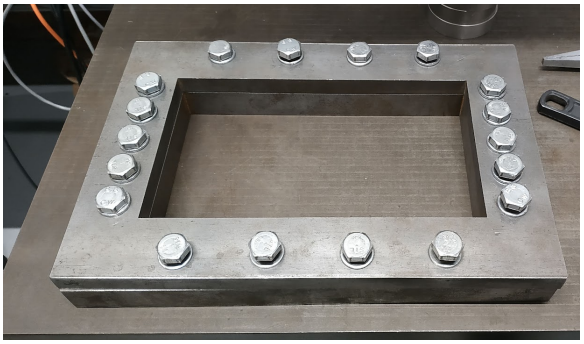

Figure 3.3: Clamp used during tests

3.1.3. Clamping

During the indentation and impact tests the panels must be held to simulate the panel being part of a larger structure such as the fuselage or wing of the aircraft. This is done via a clamp that can set the appropriate boundary conditions on the specimen, shown in Figure 3.3. In this clamp the top and bottom of the panel will be held securely with bolts whereas the sides of the panel will solely be held by the friction of the tightening of the clamp.

3.2. Testing Set-up

3.2.1. Quasi-static indentation

Most of the tests performed for the research are quasi-static indentation tests. These are done using a steel hemispherical indentor which is attached in a Zwick machine. The indentor is then lowered until a desired force, strain or work is reached. For the tests in this study mostly a desired work, or energy, was used as the parameter. The area under the force-strain curve was obtained automatically which equals to the total amount of work performed. The set-up is shown in Figure 3.4. A piece of paper can be seen on the panel which was used to identify where the indentor needed to be lined up. When the strain would increase there would have been a chance that the stiffener would be lowered onto the base of the set-up, so two metal blocks were placed under each side of the clamp to allow for this deformation without interfering with the test.

3.2.2. Ice impacts

For the ice impacts a gas gun was used to obtain the required energy levels. The gun consists of a pressure tank attached to a barrel with a release valve in between. So, instead of a desired velocity, the pressure is set for each test. Subsequently, the resulting velocity is determined afterwards using a high-speed camera and a ruler within the set-up. The complete set-up is shown in Figure 3.6. The panel is placed on its side in the clamp on the right with the barrel of the gas gun on the left.

3.3. Indentation tests

3.3.1. Analysis of stiffness distribution

To compare the impact response of the specimen to the local stiffness, the stiffness distribution was determined. This was done using an indentation distribution as shown in Figure 3.7. Every location was indented until a force of 1kN was reached. With the respective maximum displacement during this indentation the local stiffness was obtained. This test was also used to verify whether or not the

Figure 3.4: Indentation set-up

Figure 3.5: Metal blocks supporting the clamp

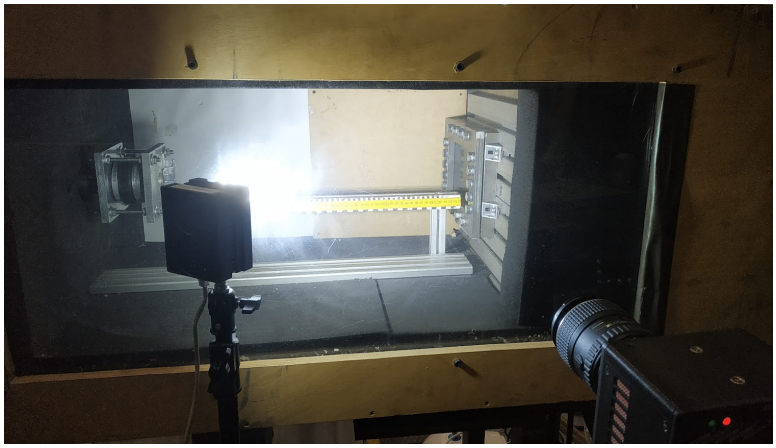

Figure 3.6: Ice impact set-up with high-speed camera and lighting

stiffener had a sufficient effect on the stiffness.

3.3.2. Effect of the stiffener

As mentioned in this chapter, the specimen were made using an Aluminium stringer along the panels. Tests were also performed to identify the effect of this stringer on the impact response of the specimen. To evaluate this effect, indents were performed at six different energy levels, as shown in Table 3.2, for both a stiffened and an unstiffened panel. The location of these indents are shown in Figure 3.8. To minimise the chance of damaged areas interfering with other indents, the higher energy levels are spread from each other. Additionally, this test was also performed on a thinner panel, made of 8 plies instead of 16 plies, again with and without stiffener. This was done to determine if the effect of the stiffener could be dependant on the thickness of the specimen.

Location	Energy[J]
1	1
2	15
3	5
4	3
5	10
6	2

Table 3.2: Energy levels at the corresponding indent locations for effect of stiffener

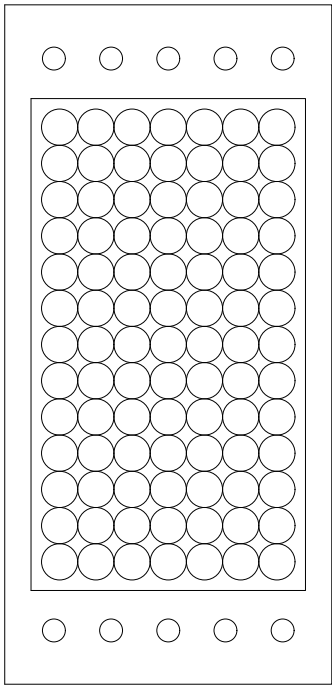

Figure 3.7: Indent overlay for the analysis of the stiffness distribution

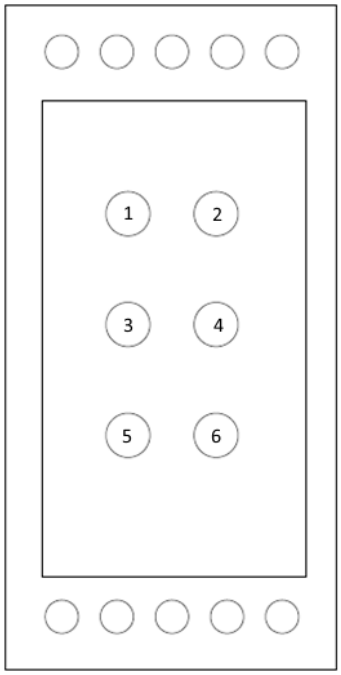

Figure 3.8: Indent overlay to determine the effect of the stiffener

3.3.3. Effect of the distance to the stiffener

For this test, the distance of the indents to the stiffener was varied at several energy levels. The aim was to evaluate the impact response with respect to the relative distance to the stiffener and thus the local stiffness. The distance to the centre line of the stiffener was varied between 0, 7.5mm, 15mm, 22.5mm and 30mm with energy levels of 3J, 5J, 10J and 15J. Again, to avoid damaged areas from overlapping, the indentation locations and corresponding energy levels are spread as shown in Figure 3.9 and Table 3.3 to Table 3.6.

In addition to this, six more locations were indented during these tests, location 6 to 11 in Figure 3.9. These were performed to evaluate the effect of the varying boundary conditions. As these indents were performed right next to the clamps and were expected to have a lower threshold energy level at which damage occurred, lower energy levels were used, namely 0.5J, 1J, 2J and 3J.

Location	Energy[J]
1	5
2	5
3	15
4	3
5	10
6-11	2

Table 3.3: Energy levels at the corresponding indent locations for the first distance to stiffener test

Location	Energy[J]
1	10
2	10
3	5
4	15
5	3
6-11	3

Table 3.4: Energy levels at the corresponding indent locations for the second distance to stiffener test

3.3.4. Distance between impacts

Another variable that was tested was the distance between two impacts. For these tests the distance between two indents was varied along the centre line of the stiffener as well as at several location along the clamps. The two indent overlays for these tests are shown in Figure 3.10 with the spacing between the impacts and the corresponding locations presented in Table 3.8. These tests were performed both at 3J and 5J along the stiffener and 2J and 5J near the clamps, with the aim to identify the effect that the stiffening of a panel can have on the potential of link-up to occur as a result of impacts.

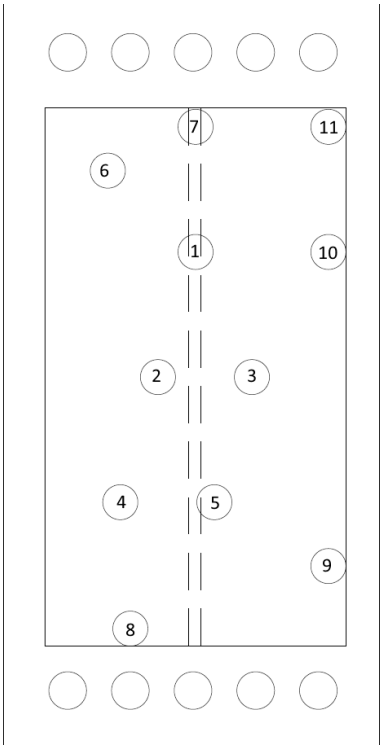

Figure 3.9: Indent overlay to determine the effect of the distance to the stiffener

Location	Energy[J]
1	3
2	15
3	3
4	10
5	5
6-11	1

Table 3.5: Energy levels at the corresponding indent locations for the third distance to stiffener test

Location	Energy[J]
1	15
2	3
3	10
4	5
5	15
6-11	0.5

Table 3.6: Energy levels at the corresponding indent locations for the fourth distance to stiffener test

Location	Spacing[mm]
1-2	0
3-4	5
5-6	10
7-8	5
9-10	5
11-12	10
13-14	10

Table 3.7: Energy levels at the corresponding indent locations for the distance between indents tests, smaller spacing

Location	Spacing[mm]
1-2	15
3-4	20
5-6	25
7-8	20
9-10	20
11-12	25
13-14	25

Table 3.8: Spacings at the corresponding indent locations for the distance between indents tests, larger spacing

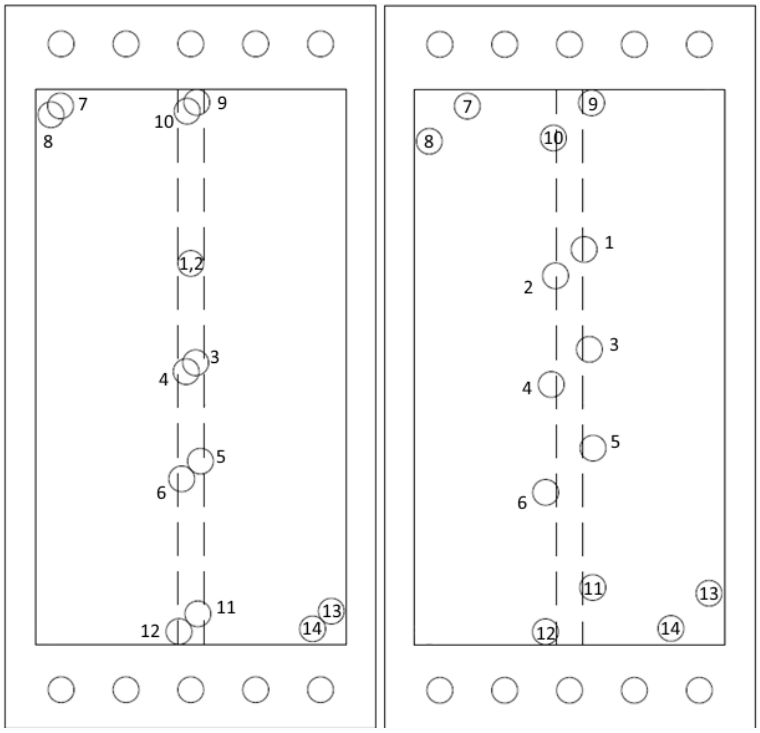

Figure 3.10: Indent overlays testing the effect of the distance between two indents with smaller spacing left and larger spacing right

Test	Spacing[mm]	Energy[J]
1	10	0.5
2	7.5	0.5
3	5	0.5
4	10	1
5	7.5	1

Table 3.9: Spacing and energy levels for the five test with repeated impacts at low energy levels

3.3.5. Repeated impacts at low energy levels

The final tests performed were the repeated indents at lower energy levels. These were done to determine the potential danger of repeated impacts in close vicinity of each other. The distribution of indents used is shown in Figure 3.11. A hexagonal pattern was made in the centre of the specimen and a rectangular pattern was used along the centre line at the side of the clamp. During these tests, the spacing between the indents was varied and energy levels were chosen around and below the threshold levels at which damaged occurred in the other tests. The resulting spacings and energy levels that were used are presented in Table 3.9.

3.4. Ice impacts

To further analyse the potential danger of hail impacts and gain an insight in the energy transfer of ice to CFRP panels, ice impacts have been performed. These tests were performed on the panels after the indentation tests. The performed tests can be found in Table 3.10 with the corresponding impact locations as shown in Figure 3.12. These location were determined to be the most critical for the indentation test, along the clamp and on the stiffener.

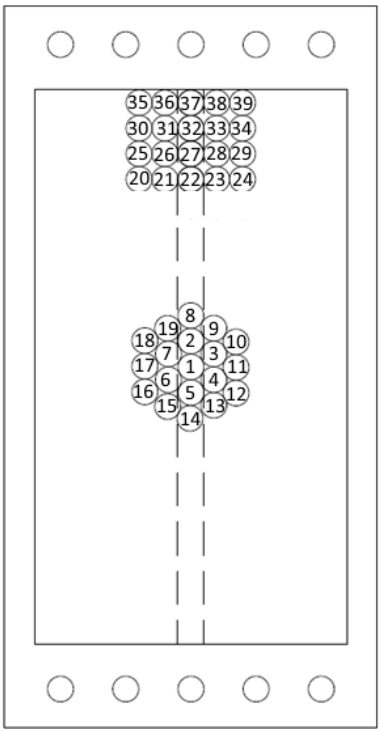

Figure 3.11: Indent overlay for the repeated indents at lower energy levels

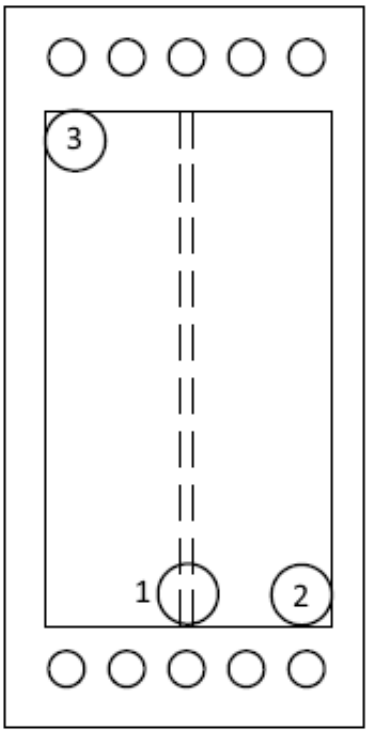

Figure 3.12: Impact overlay for the ice impacts

Test	Diameter[mm]	Kinetic energy[J]	Location	Previous indentation tests
1	15	20	1	Repeated impacts test 2
2	15	25	1	Repeated impacts test 2
3	15	22	1	Repeated impacts test 1
4	25	24	1	Repeated impacts test 4
5	25	33	1	Repeated impacts test 4
6	25	25	1	Stiffness distribution analysis
7	25	35	1	Effect of stiffener test 3
8	25	28	1	Effect of stiffener test 1
9	15	24	2	Repeated impacts test 5
10	15	25	2	Repeated impacts test 3
11	15	25	3	Repeated impacts test 3

Table 3.10: Ice impact tests

4

Results

In this chapter the results of the tests, proposed in Chapter 3, are presented and briefly discussed. More in depth analysis and conclusions are presented in Chapter 5

4.1. Analysis of stiffness distribution

The first test that was performed was to determine the stiffness distribution of the specimen. A total of 91 indents were performed until a peak force of 1kN was reached. The resulting maximum strains are presented visually in Figure 4.1, with each square coinciding with an indent location as presented in Figure 3.7. It can be seen that the stiffener had a significant effect on the stiffness as the resulting strain in the middle of the specimen resembles the values from the sides next to the clamps. Additionally, the lowest strain was found where the stiffener met the clamps at the bottom and the top. Whereas the highest strain was recorded in between the stiffener and the clamps on the sides, reaching values more than twice as high as the lowest strain.

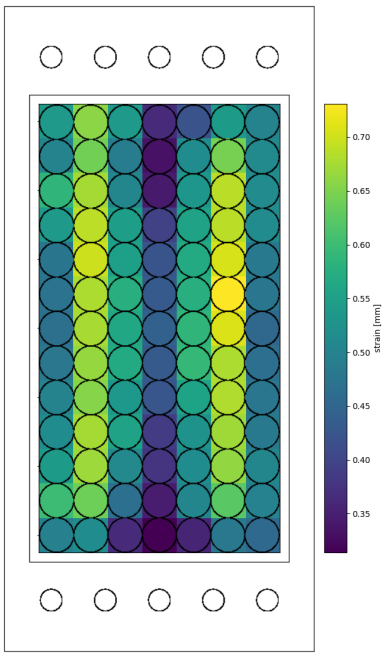

Figure 4.1: Distribution of the maximum strain at 1kN, showing the lowest strain along the stiffener and the clamps

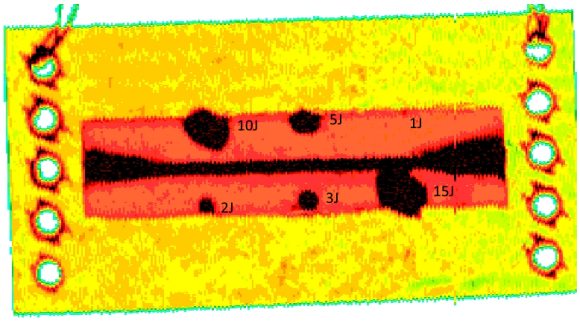

Figure 4.2: C-scan results of the stiffened panel for the effect of the stiffener

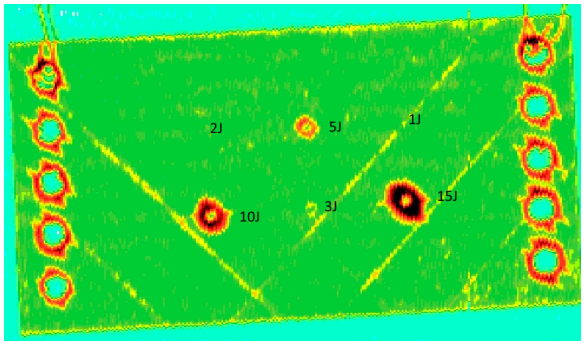

Figure 4.3: C-scan results of the unstiffened panel for the effect of the stiffener

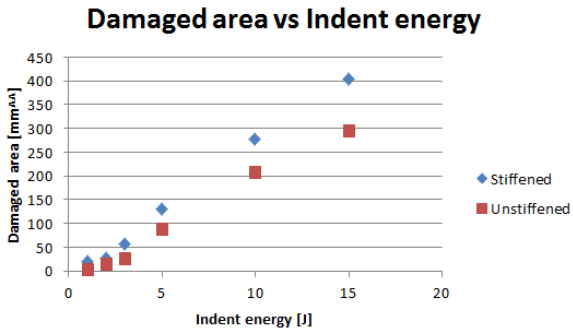

Figure 4.4: Stiffened panel consistently showing more damage compared to an unstiffened panel at all indent energy levels

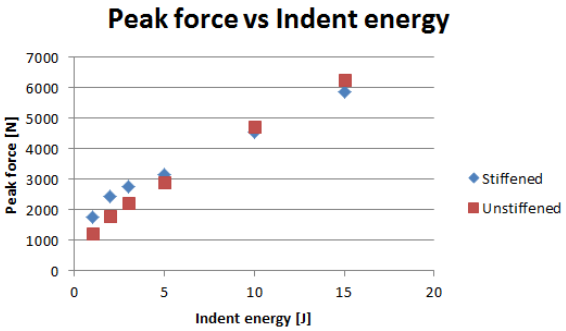

Figure 4.5: Higher peak force obtained for the stiffened panel at the lower energy levels

4.2. Effect of the stiffener

4.2.1. 16 plies

The C-scans of the stiffened and unstiffened panels with 16 plies are shown in Figure 4.9 and 4.10 respectively. The indent locations are provided with the corresponding energy levels within the picture. It should be noted that for the unstiffened panel, the indent of 2J and 10J were swapped compared to the other three tests in this category.

The damaged areas have been measured and are presented in Figure 4.4. From this figure in combination with the visuals on the C-scan it can be concluded that for all indents of the same energy, the stiffened panel shows more damage. Additionally, the damage threshold energy seems to be higher for the unstiffened panel. Where the stiffened panel shows clear damage after an indent of 2J, the first damage at the unstiffened panel can be seen at 3J.

Figure 4.5 shows the comparison of the maximum peak forces reached during the indents for both panels. For the indents up to 5J the expected results can be seen, a higher peak force is reached as the stiffened panel has a higher resistance to deformation as a result of the higher stiffness. For the indents of 10J and 15J, however, the stiffened panel shows a lower peak force. The loading curves of the 5J and 15J indents are also given in Figure 4.6 and Figure 4.7. At 5J, the result is mostly expected, a higher peak force and lower strain for the stiffened panel. But, as mentioned, the 15J indent shows a lower peak force as well as a lower strain for the stiffened panel. This is most likely due to what also caused the discontinuity in the loading curve in Figure 4.7, separation of the stiffener. The C-scan in Figure 4.9 also shows this separation as there is significant damage at the far ends of the stiffener. From the loading curves it can be concluded that these separations likely occurred during the higher energy indents and caused a sudden drop in stiffness and thus the force. Another difference between the stiffened and unstiffened panel is the energy that seems to have been absorbed by the panel in the form of permanent deformation. This can best be seen in Figure 4.6, where the strain after deloading is still almost 1mm. This is due to the fact that the stiffener used for these panels is made out of Aluminium which would more easily plastically deform that a stiffener made of CFRP.

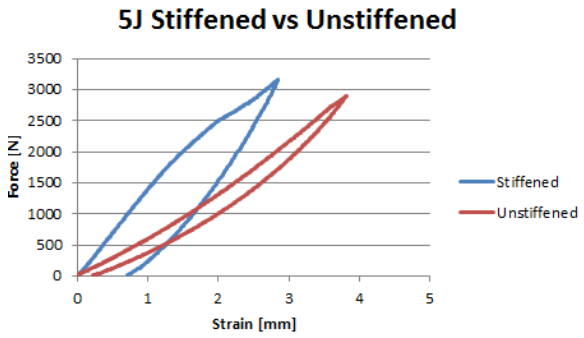

Figure 4.6: Stiffened panel results in a higher peak force and lower strain compared to an an unstiffened panel

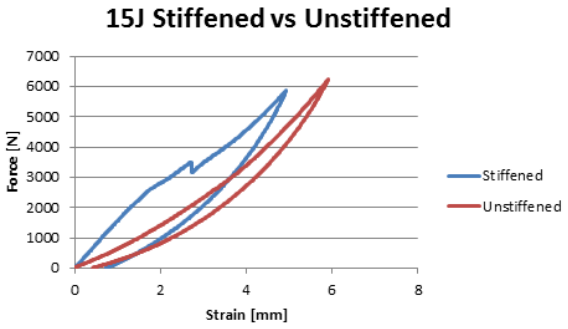

Figure 4.7: Due to separation of stiffener the stiffened panel results in lower peak force and strain than the unstiffened panel

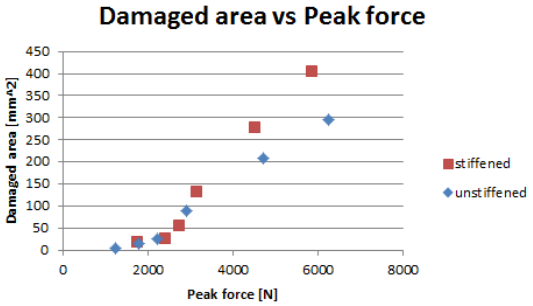

Figure 4.8: Damage formation appears to consist of two linear phases

For both panels the damaged area and corresponding peak forces are presented in Figure 4.8. For the lower energies up until 5J it can be seen that both panels behave quite similarly. Again, the 10J and 15J indent results vary from this trend, with more damage at comparable peak forces which is probably explained by the separation of the stiffener. But even including the higher energies the figure shows that the damage as a result of the peak forces consist of two phases, both seemingly linear. First a flat curve, during which relatively little damaged is formed with increasing peak force. But at a certain point, around 2500N during these tests, the steepness is greatly increased and now an increase in peak force will significantly increase the resulting damage. An important observation here is that for the unstiffened panel, the first three indents of 1J, 2J and 3J are along this shallow line, but for the stiffened panel only the 1J and 2J indent are in this part and the 3J already shows a considerable increase in damage with a relatively small increase in peak force.

4.2.2. 8 plies

The effect of a stiffener on a panel on the response to an indent was also evaluated on a thinner panel, made of 8 plies. The C-scans of these panels after the test are presented in Figure 4.9 and Figure 4.10.

For the most part, similar results can be seen compared to the thicker panel of 16 plies. Again, a significant separation can be seen at the sides of the stiffener, which were likely initiated by the indents at the higher energy levels. The damaged area and peak forces for each energy level are presented in Figure 4.11 and Figure 4.12, respectively. These graphs largely resemble the graphs obtained from the tests on the thicker panels, with the stiffened panel showing more damage and a higher peak force at the same energy, except for the indents of 10J and 15J. For these indents again a higher peak force was recorded. Figure 4.13 and Figure 4.14 show the loading curves of the indents at 2J and 10J respectively. The indents at 2J show how the stiffness of the stiffened panel cause a higher peak force and resulting a lower maximum strain, whereas the indents at 10J caused the stiffener to separate resulting in a discontinuity in the loading curve with a lower peak force and lower strain as a result.

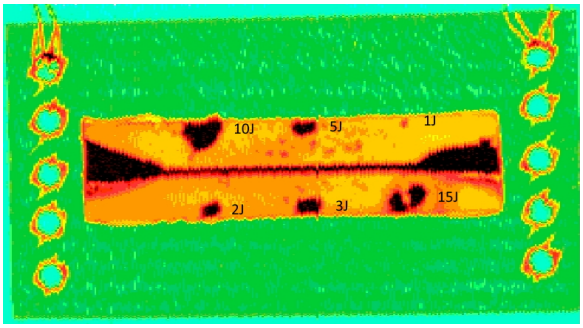

Figure 4.9: C-scan results of the stiffened panel with 8 plies for the effect of the stiffener

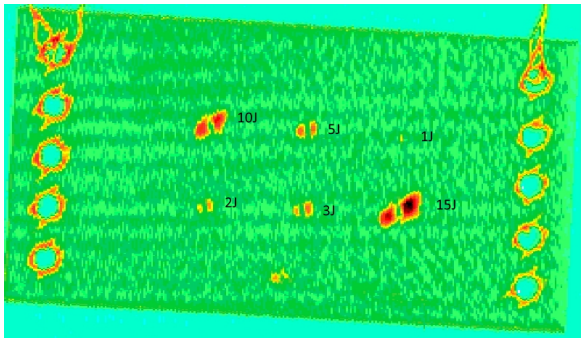

Figure 4.10: C-scan results of the unstiffened panel with 8 plies for the effect of the stiffener

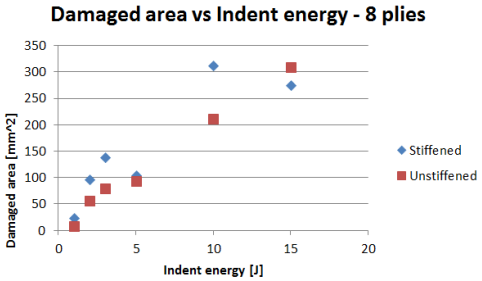

Figure 4.11: A higher damaged area is observed on the stiffened panel for most indents compared to the unstiffened panel

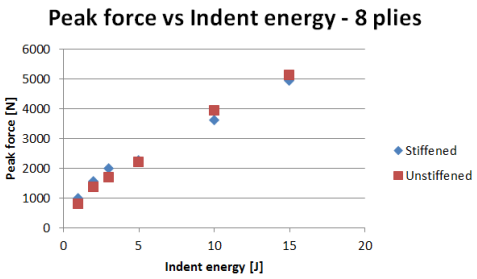

Figure 4.12: Damage as a result of peak force behave similarly for the unstiffened and stiffened panel

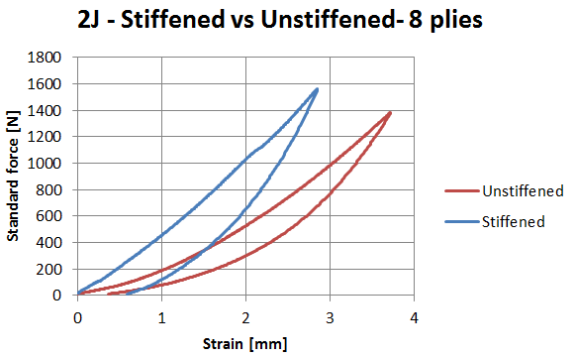

Figure 4.13: Stiffened panel results in a higher peak force and lower strain than the unstiffened panel with 8 plies

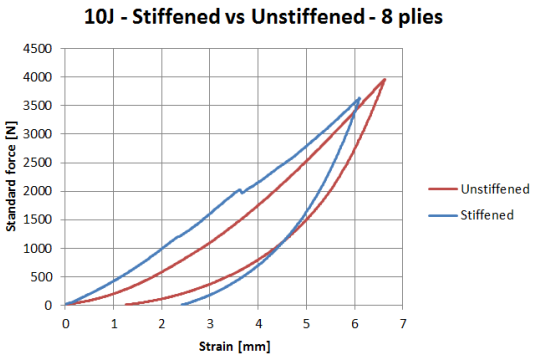

Figure 4.14: Due to separation of stiffener the stiffened panel results in lower peak force and strain than the unstiffened panel with 8 plies

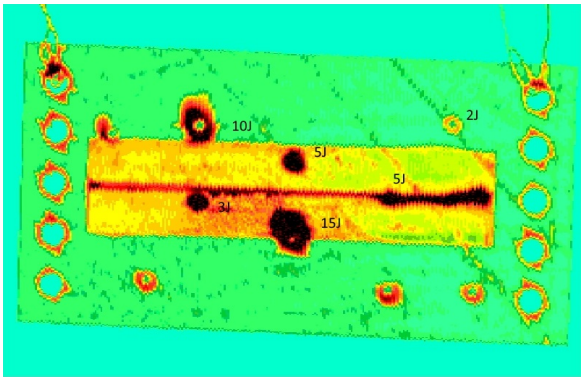

Figure 4.15: C-scan results of the first distance to stiffener test

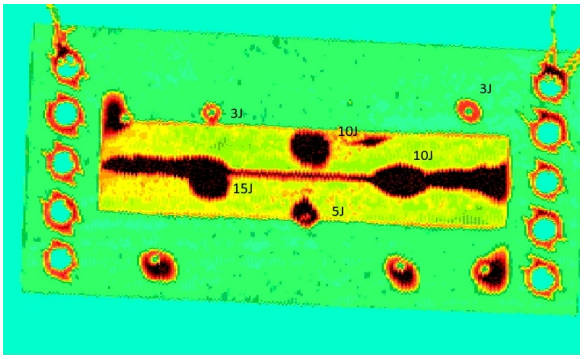

Figure 4.16: C-scan results of the second distance to stiffener test

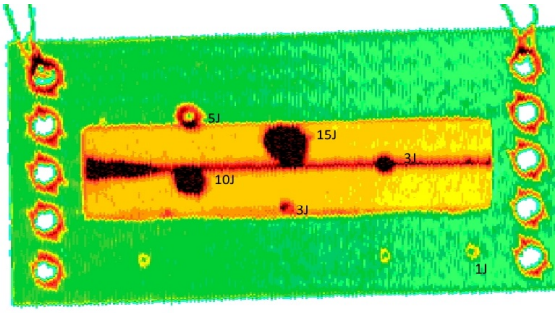

Figure 4.17: C-scan results of the third distance to stiffener test

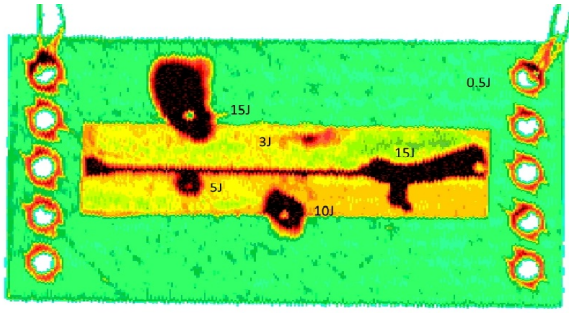

Figure 4.18: C-scan results of the fourth distance to stiffener test

4.3. Effect of the distance to the stiffener

The analysis of the distance to the stiffener and the indents near the clamps are discussed separately in the following two subsections.

4.3.1. Distance to the stiffener

The C-scans of the four panels used for the test are shown in Figure 4.15 to Figure 4.18. Again, the energy of the indents is included next to the corresponding locations. Visually, the most notable results are how the 10J and 15J indents interact with the boundary conditions. This is especially clear in Figure 4.16, with the separation of the stiffener at both sides and in Figure 4.18, with the separation of the stringer and the massive delamination as a result of the 15J indent closest to the side of the panel.

To compare the locations at different distances to the stiffener, the local 'stiffness' is used. This was determined by interpolating the strain obtained at the stiffness distribution in Section 4.1, after which the stiffness was computed by taking the inverse of the interpolated strain.

Using this local stiffness, Figure 4.19 shows the relation found between the damaged area and the local stiffness for the four energy levels. For clarity in this figure, the substantial delamination towards the side of the panel in Figure 4.18 has been removed. In practically all of these tests the results do not represent what was expected. All four tests show the greatest damage where the stiffness was the lowest, furthest away from the stiffener. Although a trend is far from conclusive from these four curves, if anything the damage seems to decrease with increasing stiffness. Additionally, the damaged areas of all the tests are compared to the corresponding peak forces in Figure 4.8, which also includes the results from the test for the effect of the stiffener. It can be seen that the four performed tests compare similarly to the previous test albeit with a lot of spread towards the higher energy levels. So, although these test do not confirm the original hypothesis, they do show that the damage is strongly correlated to the boundary conditions, such as the clamps near the indents, with the massive delamination in Figure 4.18 as an example of the interaction with the side clamp.

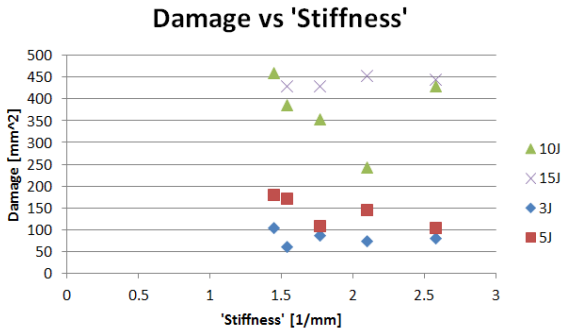

Figure 4.19: No clear trend observed comparing the damage to the local 'stiffness'

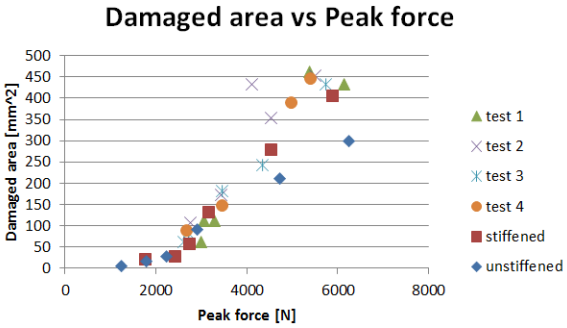

Figure 4.20: Relations between damage and peak force of the four tests in distance to the stiffener are in line with previously discussed results

4.3.2. Varying boundary conditions at low energy

In addition to the five indents performed to compare the effect of the distance to the stiffener, six more indents were performed on each panel. These were spread out at varying locations close to the clamps. The energy levels are also shown in Figure 4.15 to Figure 4.18.

No damage was found after the indents at 0.5J, but at 1J some damage can be observed, shown in Figure 4.17. Interestingly, damage did not occur at all locations. The indent at location six, corresponding to Figure 3.9, did not result in any damage. All other indents are right next to the clamps on either or even both sides. However the location without damage was located slightly away from the side. Then for the indents at 2J and 3J damage is seen in all locations with the damage being greatest next to the clamps. So as found before, the clamps in this case not only increased the damage at a certain energy level, but they also lowered the energy threshold at which damage was initiated.

4.4. Distance between impacts

The analysis of the distance between the indents along the stiffener and the indents near the clamps are discussed separately in the following two subsections.

4.4.1. Along the stiffener

Figure 4.21 and Figure 4.22 show the smaller and larger spacing of the 3J indents along the stiffener. Additionally, Figure 4.23 and Figure 4.24 show the smaller and larger spacing of the 5J indents along the stiffener. Firstly, the level of separation of the stringer seen in Figure 4.22 means that very little conclusions can be drawn from the damage underneath. What can be seen, however, is that for both the 3J and 5J indents, two indents in the same location show more damage than when these two indents are slightly further apart. This is unexpected as it goes against the hypothesis of this test and the previous research [26].

Although the resulting combined damage does not seem to exceed the indents on the same location, some link-up can be observed in several locations. for the 3J indents, link-up can be seen on the third location in Figure 4.21. Similarly, Figure 4.24 potentially shows how the first of the three locations along the stiffener shows a damage pattern corresponding to two separate indents with a connecting area in between them. It should be noted here, however, that as this damage is along the stiffener, it is difficult to separate delaminations in the CFRP from separation of the stiffener.

4.4.2. Next to the clamps

Similarly to along the stiffener, Figure 4.23 and Figure 4.22 show the smaller and larger spacing of the 2J indents along the clamps respectively. And Figure 4.21 and Figure 4.24 show the smaller and larger spacing of the 5J indents along the clamps. As found before the indents along the clamps show significantly more damages when compared to the indents along the stiffeners. This is made even more apparent as the 2J indents in the corners of the panel in Figure 4.23 resulted in more damage than the 3J indents along the stiffeners.

Considering link-up, these results again show a potential for it to occur. With the 2J indents it can be seen that at the smaller spacing they form a single combined damaged area, whereas the larger

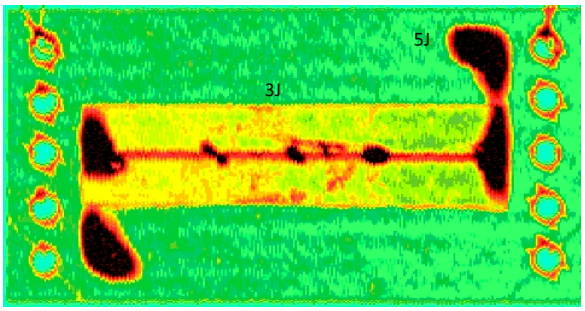

Figure 4.21: C-scan results of smaller spacing with 3J along the stiffener and 5J next to the clamps

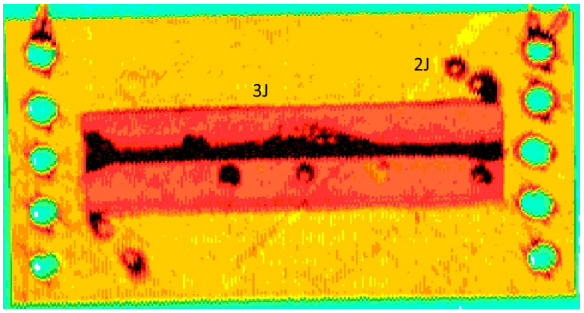

Figure 4.22: C-scan results of larger spacing with 3J along the stiffener and 2J next to the clamps

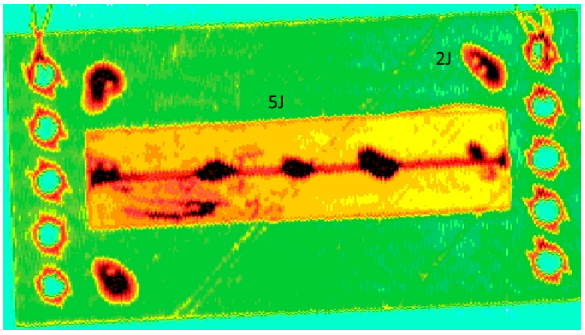

Figure 4.23: C-scan results of smaller spacing with 5J along the stiffener and 2J next to the clamps

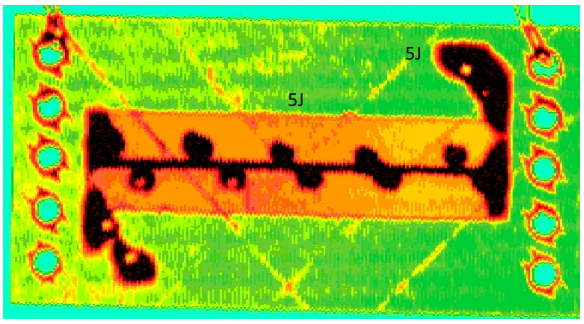

Figure 4.24: C-scan results of larger spacing with 5J along the stiffener and 5J next to the clamps

spacing resulted in two separate delaminations. Likewise, the larger spacing of the 5J indents along the clamp in Figure 4.24 show two mostly separate damaged areas in the bottom left corner, although in the top right corner the damage has linked up due to the fact that the damage as a result of a 5J indent along the clamp far exceeds that of a 2J indent in this location.

4.5. Repeated indents at low energy levels

Finally, the results of the repeated indents at a lower energy level are presented. The C-scans of all five panels are given in Figure 4.25, with the corresponding energy level and spacing between the impacts as given in Table 4.1. As all the indents and the damage is located within the area of the stiffener, only these parts are presented in the figure. It can be seen that some tests resulted in damage whereas others did not. Against the expectation, the indents that were more spread out resulted in the larger damage. With test 1, with indents of 0.5J actually showing more damage than as a result of test 5, with a smaller spacing and indents of 1J. Although test 5 does show a discrepancy in the form of a relatively large damaged area in the middle, which likely is the result of separation of the stringer.

Figure 4.26 show the damaged area in the order of the indents. While the variance is quite large, a trend can still be seen of increased damage with increasing number of repeated impacts i the vicinity. It should however also be considered that for the rectangular pattern the later indents were also closer to the clamp which can also account for the increasing damage.

Test	Spacing[mm]	Energy[J]
1	10	0.5
2	7.5	0.5
3	5	0.5
4	10	1
5	7.5	1

Table 4.1: Spacings and energy levels for the five test with repeated impacts at low energy levels

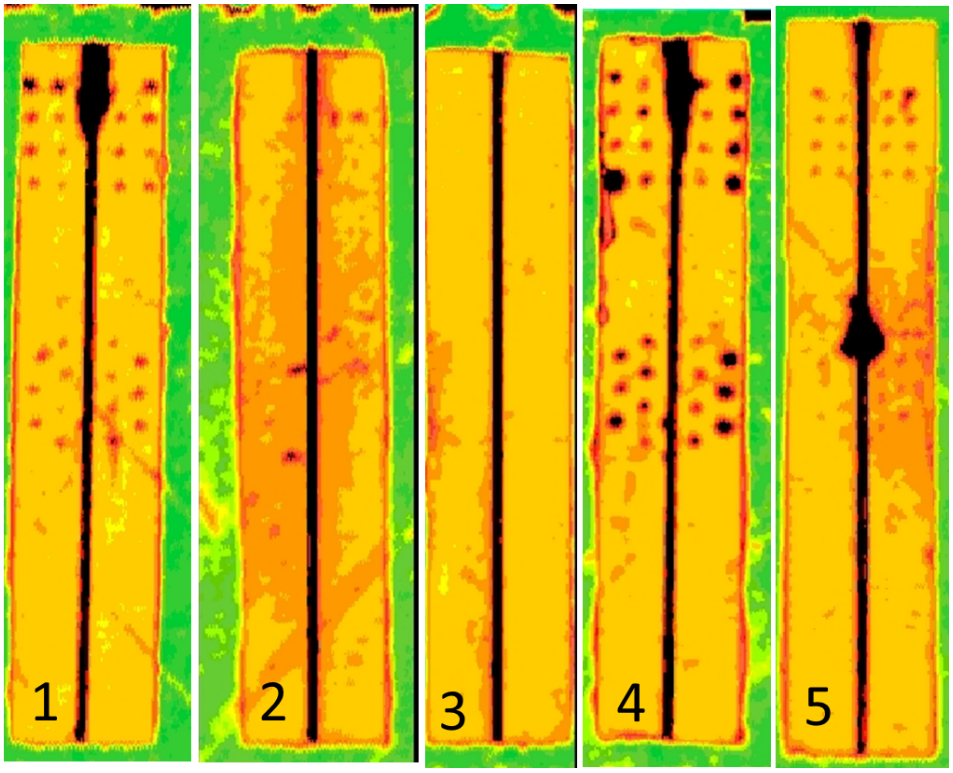

Figure 4.25: C-scan results of the five test with repeated impacts at lower energy

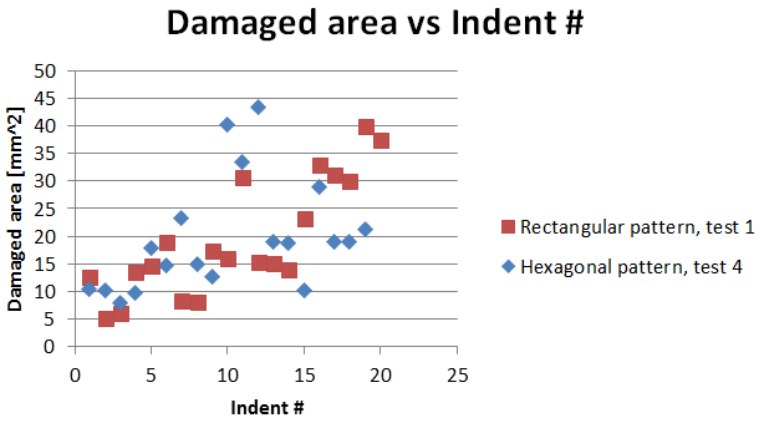

Figure 4.26: Repeated impacts showing a slight, but inconsistent, trend towards increasing damage.

4.6. Ice impacts

During the ice impacts eleven impacts were performed on a total of eight panels, according to Table 3.10. Of the eight panels only three showed any additional damage after the impacts. These three panels are shown in Figure 4.27, with the damage resulting from the ice impacts circled in red. The only damage that was observed was the small separation of the stringer at the bottom of the panel. So, the only panels where damage was observed after impacts were panels with previous damage from the repeated impacts that were then impacted at the end of the stringer next to the clamps.

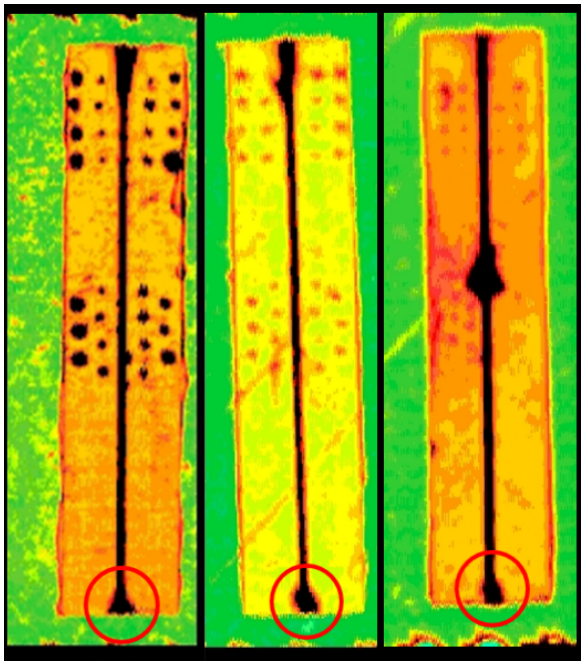

Figure 4.27: C-scan results after ice impacts showing damage circled in red. C-scans after test 1 and 2 (left), test 3 (middle) and test 4 and 5 (right).

4.7. Energy level verification

Impacts are often performed using a drop tower, where a mass is dropped from a certain height in order to transform the potential energy to kinetic energy which results in the impact energy. For this research, however, indentations were used. The press machine used for these tests keeps track of the energy using the force-displacement curve. When the programmed energy level is reached the deloading begins. But, the press and thus the indentor does not stop immediately as it takes a certain amount of time to decelerate it, causing an overshoot in energy. So, to verify that this overshoot is at an acceptable level, it was determined for several tests.

Similar to how the press machine determines the energy, the verification is done by integrating the force-displacement curves from the data of the tests. Firstly, Figure 4.28 shows the overshoot in a percentage of several tests with several energy levels. It can be seen that the overshoot is significantly larger for the lower energies, as the overshoot in strain was relatively higher for these indents. Additionally, Figure 4.29 shows the overshoot during the repeated indents at lower energy levels, for both a test at 0.5J and one at 1J. The figure shows comparable levels of overshooting as the other tests at lower energy levels. Although the overshoot for energy levels below 2J are not insignificant, they are deemed as acceptably low, with the highest energy for a 0.5J indent being an indent of 0.54J.

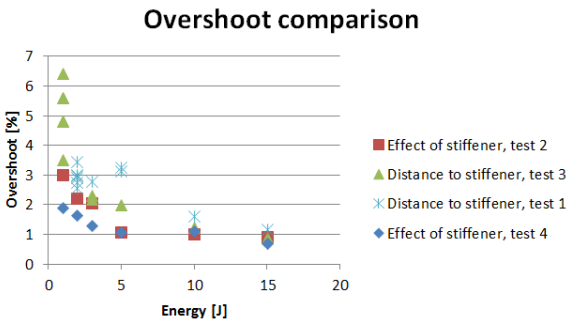

Figure 4.28: Comparison of overshoot in several tests with varying energy levels

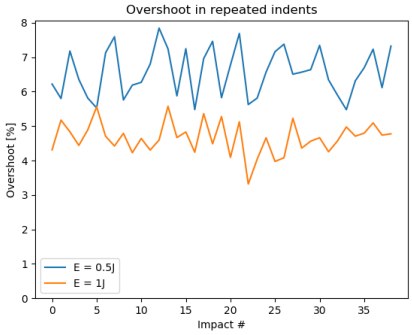

Figure 4.29: Overshoot during the repeated indents at lower energy

5

Discussion

5.1. Effect of stiffening of a panel

Several tests have been designed and performed to evaluate the effect of stiffening on a panel when indented or impacted. The most conclusive results were observed when comparing a stiffened panel and unstiffened panel when indented with the same energy at the same locations. At all energy levels ranging from 1J to 15J, more damage was created on the stiffened panel. Additionally, the threshold level at which damage first occurred was lower on this panel. These results directly confirm the proposed hypothesis that the suppression of deformation caused by the stringer results in more energy dissipation in the form of damage.

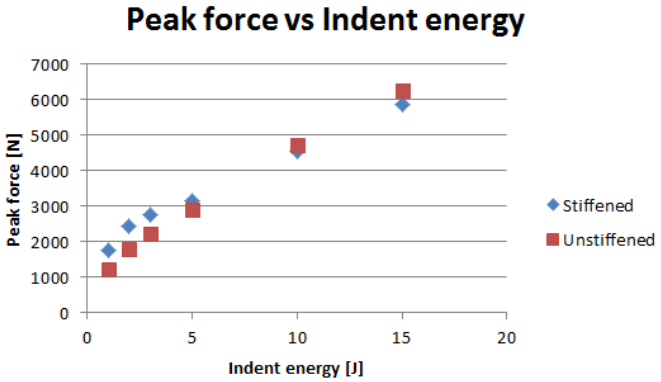

Figure 5.1: A higher damaged area is observed on the stiffened panel for most indents compared to the unstiffened panel

Another expectation was that stiffening would cause a higher peak force at the same energy level while reaching a lower strain. However, when the peak force of every indent is presented with respect to the dent energy, as shown in Figure 5.1, the results are not quite consistent. For the indents of 10 and 15J the peak force as well as the maximum strain was higher for the unstiffened panel. Looking at the loading curves and C-scans, presented in Figure 4.7 and Figure 4.9 respectively, this is attributed to the separation of the stringer. During the indentation, the stringer separated partially, which is seen in the loading curve as a sudden drop in force resulting in a lower peak force during the test. All other loading curves for the indents below 10J, such as Figure 4.6, show how the increased stiffness results in a higher peak force. The fact that the stringer separated during the indents at higher energy levels, is not something that should occur in an actual aircraft, especially not at these relatively low energy levels. It must be concluded that the adhesive was not properly applied for the performed tests. While these results do show how an impact near a previously weakened part can result in far greater damage than normally, the resulting trend in peak force and separation are not to be expected in actual aircraft. therefore, when analysing the results from the indents below 10J, it is concluded that the stiffening elements on a panel will increase the peak force and corresponding damage as the deformation is suppressed.

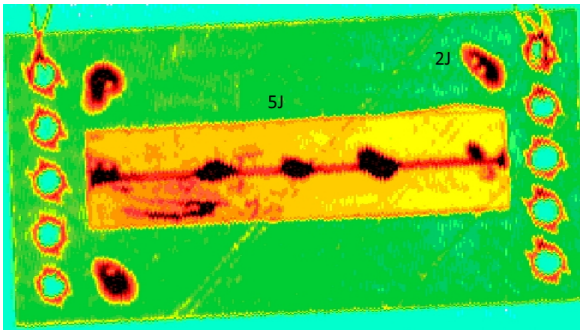

Figure 5.2: C-scan results of the third distance to stiffener test

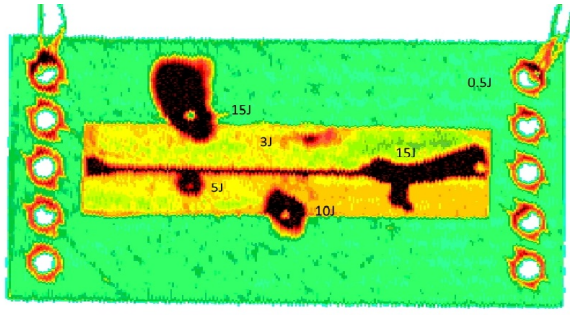

Figure 5.3: C-scan results of the fourth distance to stiffener test

The initial analysis of the stiffness of the specimen with a stringer along the center line, presented in Section 4.1, resulted in the desired stiffness distribution. The highest stiffness was observed where the clamps met the stringer and along the stringer the stiffness was higher than the locations away from both the clamp and the stringer. From this distribution it would have been expected that locations along the center line would be most prone to damage from indentations. It was observed, however, that this distribution does not provide the complete picture needed to predict the critical locations on the panel. While the stringer seemingly provides the highest local stiffness, at least during an indent up until 1kN, during the tests it was observed that the clamps on the outside were the main driving factor for damage. Figure 5.2 shows that more damage was created by two indents of 2J on the corners of the specimen right by the clamps than when two indents of 5J were performed along the stringer. Another example of the effect of the clamps is shown in Figure 5.3. The indent of 15J, furthest away from the stringer, caused a massive damaged area that appears to have spread towards the clamp. A total of five indents were performed with 15J at varying distance to the stringer, with this indent being the furthest away but resulting in the most damage. Although these results are not initially in line with the stiffness distribution obtained in Section 4.1, they do reiterate that stiffening will strongly influence damage formation as result of an indent or impact. Additionally, as mentioned, the stiffness distribution was determined by performing an indent up until 1kN which equaled to an energy level of about 0.2-0.3J, much lower than any indents performed in all other tests. So, it is possible that for tests with larger forces and more importantly, larger strains, the stiffness of the clamps will govern the local stiffness. For an actual aircraft this means that the locations where the deformation is most strongly suppressed, for instance where stringers and ribs meet, most damage can be expected from impacts.

5.2. Ice impacts

5.2.1. Impact tests

The C-scans presented in Section 4.6 show very little damage was observed as a result of the ice impacts. Only three of the eight impacted panels showed any additional damage compared to the scans after the indentation tests. The damage that was observed were all corresponding to location 1 on Figure 3.12, along the clamp on the stringer. Judging by the shape and location of the damage, however, it is concluded that the damage is most likely a separation of the stringer from the panel as opposed to internal damage in the CFRP panel such as a delamination, similar to the damage in these locations shown in Figure 4.23.

5.2.2. Energy absorption

Another important aspect to evaluate the potential danger of hail impacts is to determine the energy that is absorbed during an ice impact. As opposed to indents or impacts with steel impactors, ice will break resulting in a substantial amount of energy being lost in the fracture instead of being absorbed by the CFRP panel. Because of this, it is necessary to be able to estimate how much of the kinetic energy will actually be absorbed during the impact compared to an impact with steel.

The five impacts resulting in damage are summarised in Table 5.1, where impact 2 and 5 were performed on the same panel and location as impact 1 and 4, respectively. The damage after these

impacts is shown in Figure 4.27, which as mentioned in the previous section is comparable to the damage observed in Figure 4.23 in these locations where two indents at 2J were performed close to each other.

Test	Diameter [mm]	Kinetic energy [J]
1	15	20
2	15	25
3	15	22
4	25	24
5	25	33

Table 5.1: Diameter and kinetic energy of ice impacts resulting in damage

Comparing the results from the indents at 2J and these impacts, it would indicate that an absorption rate of 8-10% was obtained, with an outlier of 6% in test 5. This outlier, however, can be addressed by looking at the images of the ice spheres with a diameter of 25mm. Still frames moments before impact of ice spheres with a diameter of 15 and 25mm are shown in Figure 5.4 and Figure 5.5, respectively. The ice spheres with a diameter of 15mm were shot from a plastic tube which was inserted into the impact gun which fitted well and resulted in an undamaged and insulated ice sphere. In the still frame it can be seen how the ice sphere is still intact. The 25mm ice spheres, on the other hand, were inserted straight into the metal barrel of the impact gun which resulted in a broken ice sphere during the impact for most of the tests, as can be seen in Figure 5.5. The image is slightly blurry due to the water vapour as a result of the melting of the ice in addition to several pieces of debris that can be seen flying around the ice sphere. This has several reasons which are connected to the fact that the metal barrel of the impact gun was slightly too narrow for the ice spheres. As the barrel was quite narrow, there was more contact with the ice and the metal, increasing the rate at which the ice melted as well as increasing the damage on the surface as the ice sphere was pushed through the barrel. Then, the initial damage combined with the pressure during the impact resulted in the ice sphere breaking, thus reducing the actual kinetic energy with which the panel was impacted. Additionally, as the sphere was no longer intact, its resistance to fracturing further will have been lower meaning the energy absorption of the final part will have been lower as well.

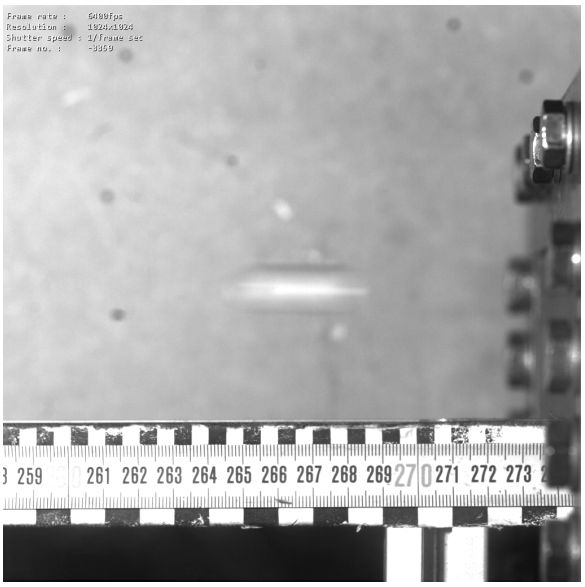

Figure 5.4: Still frame of ice sphere with a 15mm diameter before impact

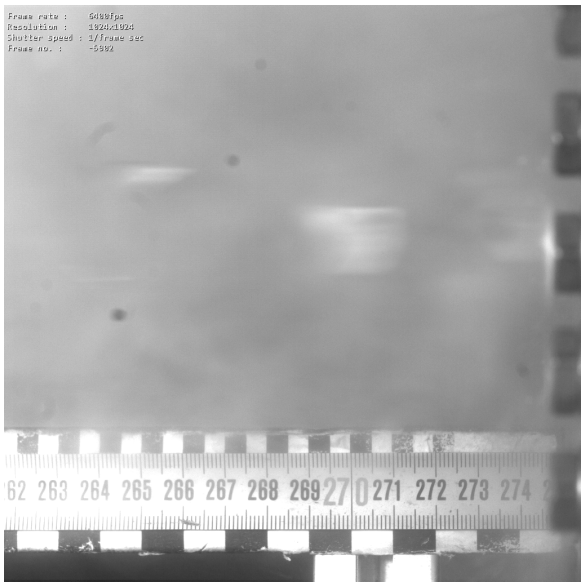

Figure 5.5: Still frame of ice sphere with a 25mm diameter before impact

To verify the obtained energy absorption, data from previous research is evaluated. In this case, data from ice impacts performed on a steel block connected to a spring and an accelerometer performed by S. Ganesh Ram is used [20]. From the data, the peak force and maximum displacement is obtained

which is used to estimate the absorbed energy. It is assumed that a linear progression is followed in the force-displacement curve for these tests, corresponding closely to the curves shown in Section 4.2. The results of this analysis are shown in Figure 5.6.

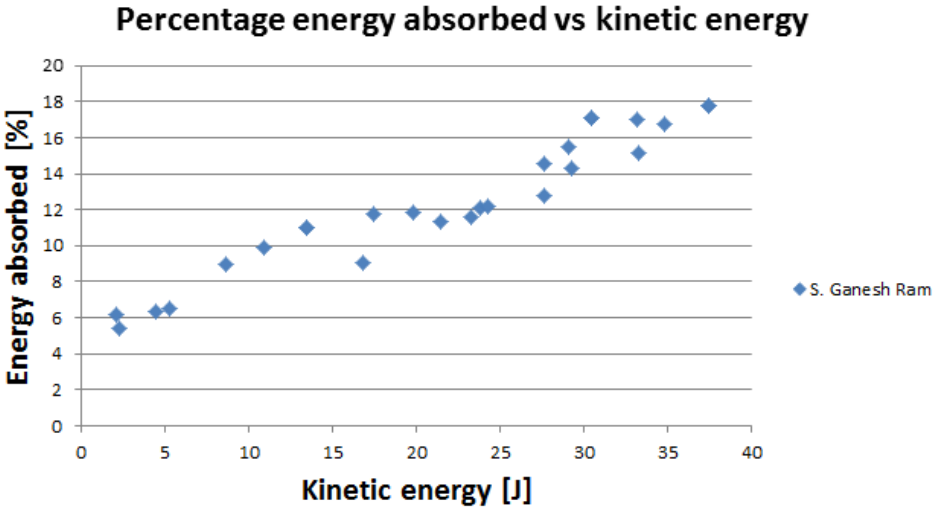

Figure 5.6: Ice impacts by S. Ganesh Ram show energy absorption is not constant for different impact energy levels

From the figure it is clear that the percentage of energy that is absorbed as a result of the impact is not constant but in fact dependant on the initial kinetic energy. This indicates that the fracture mechanics of ice spheres can behave quite differently depending on the velocity and perhaps the size. For the kinetic energy comparable to the tests performed in this study, ranging mostly from 20J to 25J a percentage of around 12% is computed. Thus, in combination with the equivalent damage observed after the indentation tests, an absorption of 10% is determined to be a good indication for further analysis.

5.2.3. Hail

The previous sections show that damage can be formed by ice impacts and the corresponding kinetic energies have been established. The kinetic energy used in the tests, however, can not be naturally reached by hail stones of the same size as the ice spheres used in the tests as the required velocities lay above the terminal velocities, as determined in Section 2.4. In this section, the potential kinetic energy of a hail stone is computed by determining the terminal velocity, density and mass of hail stones depending on the size. The results are given in Figure 5.7 up to a diameter of 55mm.

From Figure 5.7, the required hail stone diameter to reach a certain kinetic energy can be obtained. In Table 5.2, four energy levels of interest are presented with the corresponding realistic hail stone sizes. 0.5J and 1J were often found to be cut-off energy levels during the indentation tests depending on the location of the indentation. 20J was observed to be around the cut-off kinetic energy level during the ice impacts performed in this study. And finally, 5J is an energy level that showed damage in all indentations independent of its location.

Absorbed energy [J]	Kinetic energy [J]	Required diameter (with gust-without gust)
0.5	5	28mm-30mm/1.1in-1.2in
1	10	34mm-36mm/1.3in-1.4in
2	20	41mm-43mm/1.6in-1.7in
5	50	52mm-54mm/2.0in-2.1in

Table 5.2: Realistic hail stone sizes and corresponding kinetic and potentially absorbed energy levels

To evaluate the risk of these hail stones, the previously obtained data from hailpads presented in Section 2.4 is used. Figure 5.8 shows the maximum hail size distribution of around 20,000 hailpads over the span of 1999-2014. Additionally, from the damage tolerance overview of the A350 design program it was stated that the design was based on a meteorological survey. of which the following

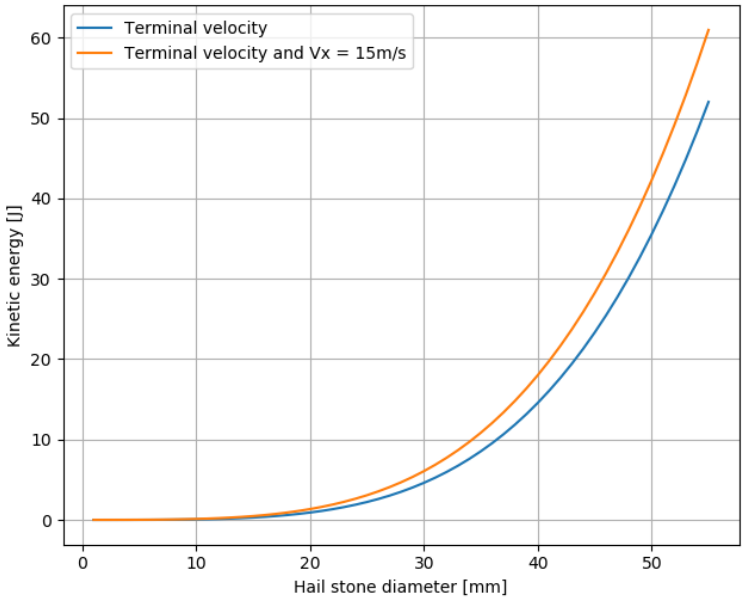

Figure 5.7: Relation between hailstone diameter and kinetic energy

sizes and distributions were retrieved[19]:

- Standard hailstorms, diameter of 10mm for 50 percent of hailstorms
- Rare hailstorm, diameter of 25mm for 5 percent of hailstorms
- Extremely rare hailstorm, diameter of 50mm for 0.1 percent of hailstorms

The maximum hail size distribution along with the data used by Airbus it can be concluded that the hail stones required to damage aircraft are not a common occurrence, but are also not at all unthinkable. According to Figure 5.8 about 4% of the hailpads had a maximum hail stone size greater than 31.8mm, which would be equivalent to an impact of at least 5J. Furthermore, about 2% and 0.8% of the hailpads showed a hail stone greater than 40mm and 50mm, respectively. So, it should be noted that these values are quite different from the data used by Airbus, but even when using the data from Airbus, 5% of the hailstorms would have hail stones above the potential cut-off energy for damage to occur and 0.1% of the hailstorms would have hailstones reaching kinetic energies of 50J, well within the range where damage will occur. Fortunately, 0.1% of the hailstorms means these are exceedingly rare, but again, not inconceivable. Especially as EASA defines *Probable Failure Conditions* as events with a probability of the order of $1x10^{-5}$ or greater per flight hour, which are anticipated to occur multiple times in the lifetime of an aircraft [2]. Combining this with the fact that in 2021 almost 4,000 major hailstorms were recorded in the USA alone, means that these storms are happening every year[24].

5.3. Potential of repeated impacts

The goal of the tests was to identify the potential danger of multiple impacts at an energy level below the damage threshold energy for single impacts. This is a situation that is likely to occur during hailstorms, as an aircraft is not struck a single time, but countless times by hail stones varying in size and kinetic energy. Similarly to the results after the ice impacts, the repeated indents showed an inconsistent amount of damage with some panels showing a considerable amount of damage and some none at all.

The C-scans of the five indented panels are shown in Figure 4.25 with the corresponding energy levels and spacing as given in Table 4.1. As discussed in Subsection 4.3.2, indents of 2J resulted in damage at all locations, indents of 1J resulted in damage along the clamps but not in the location slightly further away from the side and none of the indents of 0.5J resulted in any visible damage. For the repeated indents, however, both panels indented with 1J show damage at all locations even

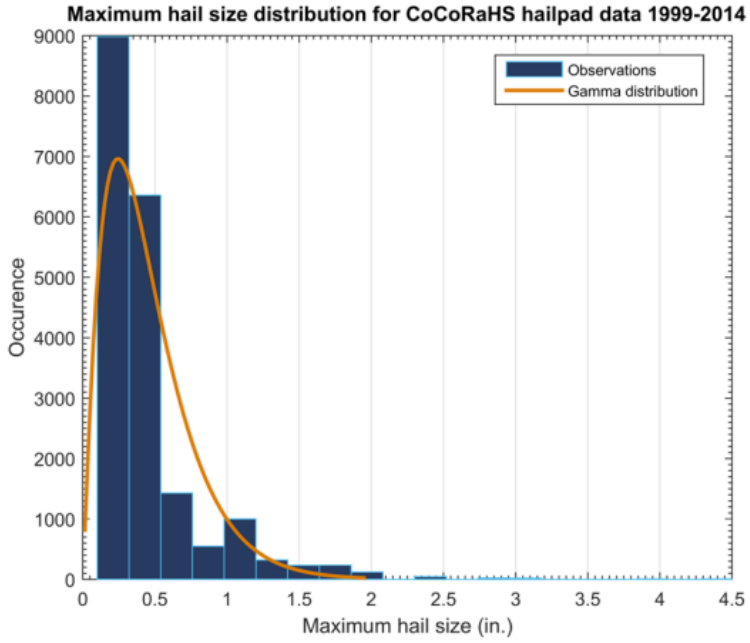

Figure 5.8: Maximum hail size distribution [11]

though these indents are not along the clamps as was the case for the damage after single indents. Additionally, one of the three panels which received repeated indents of 0.5J shows clear damage in all indent locations, while none of the single indents of 0.5J performed along varying boundary conditions resulted in any damage. These results indicate that it is a possibility that repeated impacts could be a serious threat even though the individual impacts are of a relatively low energy, around or slightly below the damage energy threshold level.

There are however several unanswered questions as a consequence of these results. The fact that only one of three panels indented with 0.5J showed any damage could have been attributed to the fact that this is around the cut-off energy level for damage to occur. However, it is questionable how for test 3 not a single indent resulted in any damage, while all locations show clear visible damage after test 1. This would indicate that there might have been another reason for the damage showing up after the first test, such as an inconsistency in the manufacturing of the specimen.

Alternatively, the spacing of the indents has a substantial effect on the damage, as this is the only difference between test 1,2 and 3. Similarly, test 4 shows substantially more damage than test 5 with only the spacing between the indents being a difference, both panels being repeatedly indented with 1J. What is most surprising here, is that the amount of damage increases with a larger spacing. For both energy levels it can be seen that the largest spacing shows significantly more damage. If there is in fact an interaction between repeated impacts, then it still needs to be answered why this interaction is greater when the impacts are spaced further apart. Likewise, it is unclear how the repeated impacts interfere with each other exactly as the damaged areas of the individual indents do not overlap or seem to have grown to each other.

5.4. Limitations of the research

While the overall results of the experiments show a clear tendency there are several limitations that were observed that should be take into account while discussing the results and future research on this topic.

Aluminium stiffener

In order to greatly reduce the complexity of manufacturing the specimen, an aluminium stiffener was attached to a CFRP panel using an adhesive. In an actual aircraft, however, the stiffeners will have been made from the same material and co-bonded or co-cured to the fuselage panel. In many tests

of this research, large separated areas between the stringer and the CFRP panel were seen in the C-scans both in and near locations of indents, such as is shown in Figure 5.9. While this could be seen as damage as a result of the indent, it is also likely that either the adhesive had not always been applied properly or the bonding method was insufficient for the forces during the tests. So, the resulting separations are not necessarily indicative of what to expect with co-cured CFRP stiffeners within an aircraft. Though it does show how a weakness, such as a manufacturing imperfection or previous small damage, can cause additional damage even when the indent or impact is not exactly on this location.

Another effect of using an aluminium stiffener is the fact that aluminium will deform both elastically and plastically. From the load-displacement curves, as shown in Figure 5.10, it can be seen for most stiffened specimen that the strain would not go back to zero after deloading. Additionally, a resulting curve could be observed visually after the test, so the specimen were strained as a result of the plastically deformed stringer. As CFRP will not deform plastically, this will have influence the load-displacement curves and potentially the amount of damage formed. The effect on the loading curve can also be seen in Figure 5.10 as a change in steepness on the curve of the stiffened panel. After around 2500N the stringer likely starts to yield, resulting in a lower steepness in the loading curve.

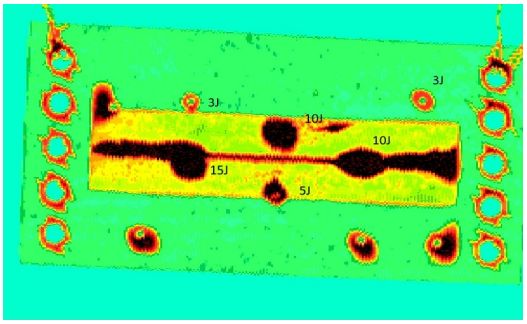

Figure 5.9: C-scan of specimen after indents, showing clear separation of the stringer on either sides as a result of the 10J and 15J indents

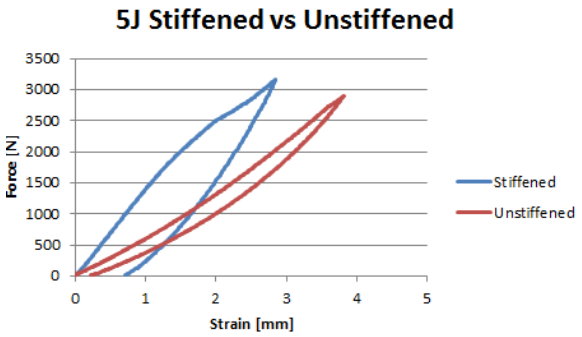

Figure 5.10: Stiffened panel results in a higher peak force and lower strain compared to an an unstiffened panel

Ice impacts

Ice impacts for this research have been performed using spheres with a diameter of 15 and 25mm. To obtain the desired energy level the outgoing velocity had been adjusted accordingly. These velocities were, however, far above the terminal velocities for hail stones of these sizes. It was determined that to reach the energy levels required for damage, hailstones with a diameter from 30-50mm are required. Even though these hailstones would then have the same kinetic energy as the ones used in this research, it is likely that hailstones of these sizes will behave differently in terms of fracture mechanics and energy transfer into the specimen. So while the ice impacts performed here are most definitely a good indication it would be beneficial to perform ice impacts with realistically sized hailstones for the corresponding kinetic energy.

Additionally, in the still frames moments before the impacts it was seen that the 25mm spheres were not intact while in the air. As a result of melting in the gas gun and the high pressure release they had fractured before impact. As a result the kinetic energy that was actually applied to the specimen was lower than what was expected. Similarly the actually energy that was absorbed by the panel will have been lower and difficult to determine. The spheres of 15mm, on the other hand, all seemed intact in the images.

Inconsistent results

Another element skewing the conclusion of the tests is the fact that the results were quite inconsistent for some parts. This was especially the case for the tests at the lowest energy levels.

The damage observed after the ice impacts has been determined to be in line with the equivalent indent damage considering the expected amount of energy to be absorbed as a result of an ice impact. This damage, however, only occurred on three of the eight panels that were impacted. The reason for this inconsistency could be vital to get a better understanding of the behaviour of hailstone impacts. It could have come from human influences, such as the creating and handling of the ice sphere before

the impact or the aiming and placing of the gun and specimen. It could also be the nature of ice that there is a variance in the internal structure during the freezing process, meaning this inconsistency will also be found in nature. Either way it was shown that ice impacts can cause damage and an estimation for the energy absorption can be made, albeit not for all ice sphere.

Similarly, when evaluating the potential for repeated impacts, three out of the five panels clearly showed damage while the other two none to very little. These indents were performed at 0.5 and 1J, which were previously determined to be around and slightly below the damage threshold level. So this inconsistency can be explained by the fact that the low energy levels are around this cut-off, meaning that slight variations in manufacturing or placement of the specimen could have been the differences in damage formation.

6

Conclusion and Recommendations

6.1. Conclusion

As a result of this study, a definitive conclusion has been drawn in determining the potential danger of impacts on stiffened panels in aircraft. In line with the current certification and testing processes, almost all previous research has focused on single, high energy impacts on unstiffened panels. Through Quasi-static indentation tests and ice impacts, this study has evaluated the effect of single and repeated impacts on a stiffened panel. Additionally, the ice impact test have given more insight in the relation between ice impacts and steel impacts, which can be used to improve future impact testing and research.

Comparing the results of the stiffened panels to the unstiffened counterparts, it was determined that the focus of the certification process of aircraft with respect to impacts should be moved to the stiffened areas, such as the locations of the frames and stringers within the fuselage. It was established that these locations proved to be the critical locations for damage to occur. Likewise, future research with respect to impacts on CFRP panels with stiffening elements must take these critical locations into account. Not only was more damage obtained with impacts of the same energy levels, but a lower energy threshold level was also observed. Thus, while a location in a free panel might show little to no damage after an impact, the same impact along a rib or stringer can seriously reduce the structural integrity.

Furthermore, this study has shown that not only single impacts must be examined, but that multiple impacts near each other have to be considered as well, both at higher and lower energy levels, as an aircraft might encounter in a hailstorm. It was observed that multiple impacts below the energy threshold at which damage was detected for single impacts, repeated impacts had the potential to cause non-negligible harm to the test specimen. Results were, however, not always consistent with the impact energy and spacing used, so further research would need to be done to evaluate the potential danger of repeated impacts at or below the damage energy threshold level. Additionally, higher energy impacts showed the possibility of link-up happening. If two impact locations are near each other the damaged areas can overlap and result in a higher overall damage as a result of the locally weakened structure.

Based on the comparison of the ice and steel impacts performed in this study and previous research, the energy levels at which ice impacts can cause serious damage on stiffened panels in aircraft were determined. It was observed that these energy levels are within the realm of possibility for hail stones recorded in real life. The corresponding hail stone sizes and resulting terminal velocities are rare. However, events with a probability of the order of $1x10^{-5}$ per flight hour are defined as *Probable* and expected to occur one or several times to an aircraft during its lifetime by manufacturers and safety regulations. As a result, these events clearly need to be considered in testing and certifying aircraft.

6.2. Recommendations

As a result of this study there are several recommendations for steps to be taken in the certification of aircraft and future research to get a better idea of the potential of impacts on aircraft.

Most importantly, the certification process for impacts needs to be revised. Impact testing needs to be performed on the most critical locations of an aircraft. While an unstiffened area might be locally weaker against compression, this study has shown that the stiffened areas along a fuselage will be the critical locations in the case of impacts. Thus all future testing and certification processes should at least include impacts in these locations.

Another recommendation is for more research to be done using ice impacts. The results observed in this study were quite inconsistent which could have been a result of ice balls breaking or melting during handling before the test. Also, while it is a close approximation, actual hail has a different construction and shape then the ice balls created in the moulds using distilled water. Therefor, the results using these ice balls will not be a perfect representation of the real life situations.

More test using ice impacts can also give a better insight in the comparison between ice and steel impactors. With this relation future testing can be done more easily and consistently if all tests can be performed using steel impactors.

In terms of testing stiffened panels, it is recommended to co-cure or co-bond CFRP stiffeners to the specimen instead of an aluminium stringer bonded using an adhesive. During this study, separation of the stringer regularly caused the results to be unclear or inconclusive as energy of the impacts was absorbed in the separation of the stringer. Using CFRP stringers also more closely resembles the situation in real aircraft, making the test more representative.

Finally, for future testing on ice impacts, it can be beneficial to perform the tests with ice balls of sizes and speeds comparable to the hail stones encountered in real life, with their corresponding terminal velocities. For this study, relatively small ice balls were impacted at high speeds to obtain higher energies. However, as ice might behave differently at different speeds and sizes during an impact, an ice ball with a larger diameter flying at a lower speed but with the same kinetic energy might show quite different results. In order to fully conclude the potential of hail storms, this would need to be evaluated as well.

Bibliography

[1] S. Abrate. *Impact on Composite Structures*. Cambridge University Press, 1998. ISBN: ISBN 0-521-47389-6.

[2] European Aviation Safety Agency. “Certification Specifications for Large Aeroplanes: CS-25”. In: Amendment 3 (2007).

[3] Airbus. “Airbus technical magazine: Special A350XWB edition”. In: *Flight Airworthiness Support Technology (FAST)* (June 2013).

[4] B. Liao et al. “Damage accumulation mechanism of composite laminates subjected to repeated low velocity impacts”. In: *International Journal of Mechanical Sciences* 182 (2020). DOI: https://doi.org/10.1016/j.ijmecsci.2020.105783.

[5] R. Alderliesten and R. Benedictus. “Fiber/Metal composite technology for future primary aircraft structures”. In: *48th AIAA/ASME/ASCE/AHS/ASC Structures, Structural Dynamics, and Materials Conference* (2007). DOI: https://doi.org/10.2514/6.2007-2404.

[6] W. Avery and D. Grande. “Influence of materials and layup parameters on impact damage mechanisms”. In: *22nd International SAMPE Technical Conference, Boston, MA* (1990), pp. 470–483.

[7] J. Baaran. “Visual Inspection of Composite Structures”. In: *EASA Research Project* (2009).

[8] A. Court and J. Griffiths. “Thunderstorm climatology”. In: *Thunderstorm Morphology and Dynamics* Kessler E. University of Oklahoma Press: Norman, USA; 9-40 ().

[9] EASA. “Hail Threat STandardisation”. In: *FINAL report for EASA* (2008).

[10] P. Guegan et al. “Critical impact velocity for ice fragmentation”. In: *Journal of Mechanical Engineering Science* 226(7) (2011), pp. 1677–1682. DOI: doi.org/10.1177/0954406211426639.

[11] I. Giammanco H. Pogorzelski and T. Brown-Giammanco. “Hailstorm characteristics: Leveraging the community collaborative rain hail and snow network hailpad damage observations”. In: *CoCoRaHS* (2016).

[12] J. Hawk. “The Boeing 787 Dreamliner: More Than an Airplane”. In: *787 Program, Boeing* (May 2005).

[13] A. Hijazi. “Introduction to Non-Destructive Testing Techniques”. In: ().

[14] R. Hohl. “Relationship between hailfall intensity and hail damage on ground, determined by radar and lightning observations”. In: *PhD final report* University of Fribourg (2001).

[15] B. Surowska J. Bieniaś and P. Jakubczak. “Influence of repeated impact on damage growth in fibre reinforced polymer composites”. In: *Eksploatacja i Niezawodnosc - Maintenance and Reliability* 17.2 (March 2015), pp. 194–198. DOI: 10.17531/ein.2015.2.4.

[16] H. Kim, D. Welch, and K. Kedward. “Experimental investigation of high velocity ice impacts on woven carbon/epoxy composite panels”. In: *Composites* Part A 34 (2003), pp. 25–41. DOI: doi.org/10.1016/S1359-835X(02)00258-0.

[17] M. Laurençon. “Impact fatigue on composite panels”. In: *Internship report, TU Delft* (September 2017).

[18] J. Le. “Hail Ice Damage of Stringer-Stiffened Curved Composite Panels”. In: *Thesis report, San Diego: University of California* (2013).

[19] E. Morteau and C. Fualdes. “Composites at Airbus Damage TOlerance Methodology”. In: *FAA Workshop for Composite Damage Tolerance and Maintenance* (July 2006).

[20] S. Ganesh Ram. “Can Hail Impacts Trigger @miscnoaa national weather service$_2$022, $title = Stormpredictioncenterannualreportsummary - 2021, url = https://www.spc.noaa.gov/climo/online/month$ $NOAANationalWeatherService, year = 2022, month = JanDelaminations$?”. In: *Thesis report, TU Delft* (August 2021).

[21] N. Razali et al. “Impact Damage on Composite Structures – A Review”. In: *The International Journal Of Engineering And Science* 3 (2014), pp. 8–20.

[22] M. Richardson and M. Wisheart. “Review of low-velocity impact properties of composite materials”. In: *Composites Part A* 27A (1996), pp. 1123–1131.

[23] M. Rout and A. Karmakar. “Low velocity impact performance of delaminated composite stiffened shell”. In: *11th International Symposium on Plasticity and Impact Mechanics, Implast 2016, Jadavpur University* (2016). DOI: https://doi.org/10.1016/j.proeng.2016.12.021.

[24] NOAA National Weather Service. *Storm prediction center annual report summary - 2021*. Jan. 2022. URL: https://www.spc.noaa.gov/climo/online/monthly/2021_annual_summary.html.

[25] Z. Song et al. “Skin-stringer interface failure investigation of stringer-stiffened curved composite panels under hail ice impact”. In: *International Journal of Impact Engineering* 122 (December 2018), pp. 439–450. DOI: 10.1016/j.ijimpeng.2018.09.014.

[26] A.J.M. Verstraeten. “Investigation of low-velocity impacts in multiple impact locations and the effect on its fatigue life”. In: *Thesis report, TU Delft* (June 2019).